Master Thesis

submitted within the UNIGIS MSc programme

Interfaculty Department of Geoinformatics - Z_GIS

University of Salzburg

Mapping land use and landcover change in Kalmar, (Sweden) using object-based change detection.

by

Marien Tijssen

U1523243

A thesis submitted in partial fulfilment of the requirements of

the degree of

Master of Science (Geographical Information Science & Systems) – MSc (GISc)

Advisor:

Dr. Gudrun Wallentin

Kalmar, 24 april 2018

Science pledge

By my signature below, I certify that my thesis is entirely the result of my own work. I have cited all sources I have used, and I have always indicated their origin.

(Place, Date) (Signature)

Abstract

The focus of this research is to map and analyse the land use and land cover (LULC) changes between 1999 and 2017 in the municipality of Kalmar, with an object-based change detection method. Studying LULC changes is important since there is a decline in agricultural lands, a growing population and an increase of urban areas. The effects of LULC changes have a bigger impact than climate change in the future. Object-based change detection between remotely sensed images has been suitable to analyse LULC changes. In this research, one Landsat ETM+ image from 1999 and two Sentinel 2a images of 2017 were classified. The research methods consisted of an object-based post-classification method, in eCognition, to detect LULC changes. To achieve higher classification accuracy, the method was combined with visual inspection and a manual re-classification of wrongly classified objects. The overlay method in ArcMap was applied to reveal the 'from-to' changes.

Four LULC classes were mapped and analysed. The overall accuracy of the classified LULC maps was 95% for the Landsat image and 95% for the Sentinel 2a image. Kappa index was 93% for both images. The maps showed that between 1999 and 2017 urban land use increased with 7 km^2 and 20%. Agricultural lands declined with 24 km^2 and -10%. Main drivers for the loss in agricultural lands were the expansion of urban areas and a growth in vegetation. The results of this study showed that object-based change detection helps to gain insight in LULC changes over time.

Keywords: object-based change detection, remote sensing, LULC, object-based image analyse,

Acknowledgements

First, my gratitude goes to my supervisor Dr. Gudrun Wallentin for the support during the process of this research and the help to gain more focus in my dissertation. Also, thanks to Dr. Josef Strobl for helpful advice in the classification part.

I also want to say a big thanks to the staff members of the UNIGIS Salzburg team. Although it was a distance-based study, they made me feel a part of the University of Salzburg. With their help, I was also able to continue my studies during the process of emigration from the Netherlands to Sweden.

Thank you, Emill Stille and Tomas Burén from the municipality of Kalmar for helping me configuring my thesis topic.

Many thanks to my loving wife Corien for believing in me during my studies. During the process of research of my master dissertation, she has been a real support. Sometimes critical, sometimes only listening when I was rambling about some issues. And of course, I want to thank my parents for raising me for the person I am and for giving me the study possibilities.

Contents

SCIENCE PLEDGE **3**

ABSTRACT **4**

ACKNOWLEDGEMENTS **5**

CONTENTS **6**

1.0 INTRODUCTION **8**

1.1 Background 8

1.2 Literature study 10

1.3 research aim and individual objectives 15

2.0 STUDY AREA, DATA AND SOFTWARE **16**

2.1 Study area 16

2.2 Data 17

2.3 Software 20

3.0 METHODS **21**

3.1 General steps of object-based change detection 21

3.2 Pre-processing 23

3.3 Image segmentation 25

3.4 Classification 27

3.5 Accuracy assessment 32

3.6 Change detection 34

4.0 RESULTS **35**

4.1 Accuracy assessment 35

4.2 Classification and map statistics 37

4.3 Change Detection 40

5.0 DISCUSSION **45**

5.1 Strengths of using an object-based classification and change detection 45

5.2 Problems of the study 47

6.0 CONCLUSION **50**

6.1 Research objectives, summary of findings and conclusions 50

6.2 Recommendations for future research 52

REFERENCES **53**

Datasets 58

APPENDICES.....59

APPENDIX A: VEGETATION OR AGRICULTURAL LANDS THAT CHANGED INTO URBAN AREAS BETWEEN 1999 AND 2017 60

APPENDIX B: UNMODIFIED FROM-TO CHANGE MAP STUDY AREA. 61

1.0 Introduction

1.1 Background

Monitoring LULC transformations is important because of the impact these changes have on climate, eco and live systems. For example, a human-driven LULC change in the form of urbanization has led to a rise in surface temperatures (Kalnay and Cai, 2003). Insight in LULC change is contributing to sustainable land management, for example in the fields of urban planning, agricultural development and climate change (Dewan and Yamaguchi, 2009, Kalnay and Cai, 2003, Wu et al., 2006). Urbanization is a human-altered driver of LULC change. According to a study by Grimm et al. (2008), the growth of the urban population led to the result that since 2010 more people live in cities than on the rural countryside. Growing urban areas are causing ecological problems and challenges in food production (Grimm et al., 2008). Urbanization is driven by economic and population growth and the improvement of infrastructure (Antrop, 2004).

Around 2100 the continuous changes on the LULC surface of the earth have a bigger impact on the environmental systems than climate change (Chapin III et al., 2000). LULC changes caused by humans is affecting several aspects of the earth such as eco-systems, freshwater resources, air quality and climate change (Foley et al., 2005). For example, deforestation in the Amazon resulted in the loss of forests and in a decrease of eco-systems (Fearnside, 2005). The surface of the earth is changing with high speed at both global and local scale, due to human-caused LULC change (Turner et al., 1994).

According to Seto et al. (2012) urban areas keep growing and until 2030 these areas will expand to 1.2 million km^2. The study notes that at this time the urban population will exceed towards 5 billion people. This continuous growth will increase the pressure on food security, ecological systems and climate. In China, urban expansion between 1992 and 2012 has led to a loss in habit and is threatening several species (He et al., 2014). In other studies, urban expansion is linked with agricultural land loss and with a rise in surface temperature (del Mar López et al., 2001, Fazal, 2000, Kalnay and Cai, 2003).

An important effect of ongoing urbanization is the loss of agricultural lands, which is affecting food production. The loss of farmlands is going fast in countries with a high pace of urbanization such as China and India (Fazal, 2000, Tan et al., 2005). As a result, in China, the loss of farmlands is threatening the overall food production (Jiang et al., 2013). The

transformation from an agricultural economy to an industry-based economy has in many countries resulted in a loss of agricultural grounds (del Mar López et al., 2001).

In Europe, urbanization is an ongoing process at high speed since the industrial revolution. Nowadays around 80% of the European population is living in urban areas (Antrop, 2004). The last decennia most cities in Europe expanded on agricultural lands (Kasanko et al., 2006). Future outlooks predict that agricultural lands in Europe will continue to decrease (Seto et al., 2013). Mainly due to a moving population from rural to urban areas, technologic development and urbanization (Antrop, 2004).

Agricultural land loss due to urbanization is not only a problem of European countries with a high population density, but also happens in less populated countries (Skog and Steinnes, 2016, Wästfelt and Zhang, 2016). In their study, Wästfelt and Zhang (2016) found out that 85% of the Swedish population is already living in urban areas. The research also showed that agricultural lands in Sweden are transformed to urban areas. With a rise in population, it is expected that urban areas will grow and put more pressure on agricultural lands.

There is a demand to monitor LULC changes such as urbanization and agricultural land loss (Antrop, 2004, Skog and Steinnes, 2016). Monitoring LULC transformations is important because of the impact that these changes have on climate, eco and live systems. Studying LULC changes can help to identify vulnerable areas where agricultural lands are under pressure. These insights in LULC changes can help to develop a more sustainable land policy (Kasanko et al., 2006).

Remote sensing has proved to be a useful instrument for mapping and monitoring LULC changes. In many studies, remote sensing images are used to gain an understanding of an altering landscape (Yuan et al., 2005, Ward et al., 2000, Shalaby and Tateishi, 2007). Remote sensing is used in studies to observe and analyse changes in urbanization, agricultural lands, landscapes and more (Brannstrom et al., 2008, del Mar López et al., 2001).

In remote sensing, change detection is often applied to study changes in the surface of the earth. Change detection is about comparing two or more temporal images of the same study area, in order to identify transformations of an object or phenomenon (Singh, 1989). The development of change detection techniques has emerged in the last decades and the topic is researched in many studies (Hussain et al., 2013).

1.2 Literature study

1.2.1 Change detection

Change detection is about comparing two or more temporal images of the same study area, to identify transformations of an object or phenomenon (Singh, 1989). Change detection techniques are used for different purposes, such as forest and vegetation change monitoring (Hayes and Sader, 2001), urban sprawl (Zanganeh Shahraki et al., 2011), LULC change (Abd El-Kawy et al., 2011), wetland change detection (Munyati, 2000), monitoring landscape changes (Taylor et al., 2000) and more. These change detection techniques are based on multi-date images acquired with remote sensing applications.

Many change detection techniques are developed in the past decennia and they are roughly divided in two approaches: pixel-based and object-based (Hussain et al., 2013). The pixel-based change detection approach is focused on the spectral difference of pixels in the same area but from different times (Lu et al., 2004). In object-based change detection, objects from different times are compared. These image objects are grouped pixels that represent objects in the real world, such as vegetation of buildings (Chen et al., 2012).

The availability of a pixel or object-based change detection approach has led to numerous studies in discussing and reviewing these techniques (Hussain et al., 2013, Lu et al., 2004, Singh, 1989). Hussain et al (2013) divided these change detection methods in the following categories: direct comparison, transformation, classification based, machine learning, GIS, advanced methods, direct object comparison based, object classification comparison based, multitemporal object and data mining. Despite the enormous amount of literature, not one single technique is suitable for every change detection application (Lu et al., 2004). In their paper, Hussain et al (2013) explain that the selection of a change detection method depends on the objectives of the research, since every method has their own specialities. Some methods only provide a binary change result for example ‘change’ or ‘no-change’ and others like, the post-classification change detection method, reveal ‘from-to’ changes (Hussain et al., 2013). Therefore, choosing a change detection method is an important part of every LULC change research.

1.2.2 Pixel-based change detection

Pixel-based change detection techniques have been used successfully for several decades to map and monitor LULC changes (Hussain et al., 2013). For example, Deng et al., (2008) applied a Principal Component Analysis technique to detect transformations in an urban environment

derived from multi-sensor and multi-temporal satellite data. They found out that several changes in land use occurred in the study area. However, the researchers used a combination of the Principal Component Analysis and supervised classification**.** The Principal Component Analysis only detects change or no-change between images. Yuan et al. (2005), used a post-classification change detection method. Four Landsat images were used to study LULC changes in the study area. First, the images were classified into six land classes. Then a post-classification comparison was applied. The method revealed 'from-to' information or in other words what was the former class and what is the present one. With this method, it is possible to calculate the loss of land classes and visualize them on a map. However, the study of Tehrany et al. (2013) reveals that the success of this method depends on the classification accuracy. The study shows that misclassifications in each image will affect the change detection result negatively. Furthermore, applying a post-classification method costs a lot of time and expertise from the analyst (Lu et al., 2004).

1.2.3 Object-based change detection

With the launch of high-resolution satellites, object-based change detection techniques for mapping and monitoring LULC changes are emerging. The object-based change detection approach has been successfully used to map and monitor LULC changes (Lefebvre et al., 2008, Hussain et al., 2013). To detect variations between objects, several statistical operators are available. Hussain et al. (2013) described three object-based change detection methods: Direct Object Chang Detection, Classified Objects Change Detection and Multitemporal/multidate-object change detection.

Direct Object Change Detection (DOCD)

Chen et al. (2012) describe that the direct object change detection method is comparing image objects from two different dates. They point out that change detection focusses on different spectral values or variances in shape, size and compactness of image objects. The downside of this method is that it is not possible to gain insight in 'from-to' information (Chen et al., 2012).

Classified Objects Change detection (COCD)

Hussain et al. (2013) explain that classified objects change detection is comparable with the pixel-based post-classification change detection method. First pixels are segmented into geographical objects, followed by classification. After classification post-classification is applied to detect changes. However, research shows that the success of this change detection method is depending on the classification accuracy and proper segmentation (Zhou et al., 2008, Tehrany et al., 2013). Objects can have different sizes, especially if different sensors are used

and these differences can affect the change detection results (Hussain et al., 2013). Just with the pixel-based post classification approach, this method is revealing 'from-to' statistics.

Multitemporal/multidate-object change detection

Hussain et al. (2013) describe that multitemporal or multidate-object change detection is about stacking two or more images from different times together. They point out that the stacked image is then segmented and classified, followed by a statistical operation to detect changes. The downside of this method is that it only detects changes based on the first image. New geographical objects that appear in the second image and not exist in the first one, will not count as change (Hussain et al., 2013).

Of all these methods, Classified Objects Change Detection is the most used (Chen et al., 2012). The development of new change detection methods will increase, especially with the fact that more high-resolution satellites will be launched.

1.2.4 Advantages of object-based vs. pixel-based change detection

The implementation of an object-based change detection method has several advantages compared to pixel-based change detection approaches. Classification is an important step when change detection is applied. Studies show that object-based classification has a higher accuracy compared to pixel-based classification. For example, the study of Yan et al. (2006) discovered that the object-based classification with medium resolution images was 33% more accurate, compared with pixel-based classification. In another study object-based classification was applied to map urban dynamics in China. An et al. (2007) found that out that - compared with pixel-based classification - the object-based approach had a higher accuracy. In their study they used Landsat Thematic Mapper data with a pixel size of 30 meters.

Another benefit of applying the object-based approach for LULC change mapping is the disabling of the 'salt and pepper' effect (Blaschke et al., 2000). The disabling of this effect is resulting in a quieter image.

1.2.5 Challenges in object-based change detection

Despite that object-based image classification achieved higher accuracies compared to pixel-based classification, object-based change detection still has its challenges:

Sliver polygons

Segmentation and object-based classification of images and then applying change detection, for example with a post-classification approach, lead to sliver polygons. Sliver polygons are a result of overlapping two or more GIS-layers and are small scattered polygons in a vector or

raster image (McDermid et al., 2008). In their study Chen et al. (2012) explain that sliver polygons are caused when images are taken at different sun angles and times. Furthermore, they are caused by misregistration, misclassifications and unappropriated segmentation (Chen et al., 2012).

Over or under segmentation

Segmentation of an image is an important part of object-based image classification. Images are segmented into heterogenous objects that have similar shape, size, spectral and textural values. Under or over segmentation is a common problem in object-based image analysis (Hussain et al., 2013). With over segmentation, geographical objects are divided into smaller parts instead of one part, whereas under segmentation is when several different geographical objects are grouped as one object (Liu and Xia, 2010). Over or under segmentation can result in misclassification, which leads to poor classification accuracy and false change detection registration (Song et al., 2005). Several researchers suggest that optimal parameters for segmentation are achieved by trial and error (Hussain et al., 2013). Despite that several researchers showed methodologies that can be applied to decrease the effect of under or over segmentation, there is still not one solution.

1.2.6 Emerging issues in change detection

Early change detection techniques were pixel-based and are steadily developing in more object-based methods. With the launch of more satellites, data availability is expanding but some challenges are also emerging.

Big data and remote sensing

The launch of earth observation satellites with high-resolution sensors such as Quickbird (0.61 m), Ikonos (1 m) and Spot-5 (2.5 m) leads to terabytes of data (Ma et al., 2015). This development is caused due to the fact that more and more people use geographic and remote sensing data for a wide range of applications. Scientists are naming these enormous datasets ‘big data’ (Philip Chen and Zhang, 2014). In the literature there are different definitions for big data. In general, it has the following characteristics: large datasets (volume) that are transferred at high speed (velocity), the datasets consist of complex and varied data (variety) (Lewis et al., 2016, Ma et al., 2015).

Big data is an emerging field in the literature and this is the same for big data in combination with remote sensing. There is large potential to use big data in remote sensing for monitoring and mapping LULC changes. On the other hand, with the current computer technologies, there

are several challenges before big data can be used regularly for remote sensing applications. There are challenges in data storage, handling of big data sets and presentation of the data (Ma et al., 2015, Nativi et al., 2015, Oliveira et al., 2012). For example, traditional storage devices are not capable of handling enormous datasets (Oliveira et al., 2012). Especially since datasets from earth observation devices are already containing terabytes of data (Ma et al., 2015). Current computers are not able to process these quantities. In their study, Li et al. (2016) explain that that traditional database structures (such as SQL) are not capable of handling big data sets. Problems are also in the visual presentation of big data (Nativi et al., 2015).

Opportunities change detection

Despite the current challenges in the use of big data in remote sensing, there are opportunities for successful implementation in earth observation applications. For example, the global scale monitoring of LULC changes is possible with multiscale and temporal datasets (Lewis et al., 2016). Also, the implementation of datasets from different sensors become easier (Giuliani et al., 2017). An example of a promising research direction is the development of a data frame for large remotely sensed datasets (Giuliani et al., 2017, Lewis et al., 2016).

The study of Lewis et al., (2016) showed that fast accessing and processing large Landsat datasets is possible. In this study, Landsat data of 27 years of the Australian continent was used in a High-Performance Data (HPD) and High-Performance Computing (HPC) setting to detect changes in surface water. This setting or data frame is named the earth observation data cube. The study shows that it was possible to analyse and measure surface water changes at high speed from big datasets derived from the Australian continent. However, the spatial scale of the data was 25 m. With high-resolution data (pixel size < 5m) the data load would be bigger and more difficult to handle for the earth observation data cube.

Developments in big data and data frameworks can lead to major possibilities in the field of LULC change detection. In the future, researchers are able to process and analyse LULC data faster and with more precision. These advances in LULC change detection will contribute to face the challenges in urbanization, the protection of agricultural lands and lead to more sustainable land planning policies.

1.3 research aim and individual objectives

1.3.1 Research aim

The aim of this study is to map and analyse the LULC changes in the municipality of Kalmar (Sweden), with an object-based change detection method.

Literature shows that there is a demand to monitor and map LULC changes (Antrop, 2004, Skog and Steinnes, 2016). The results of this study will help to provide insight into the LULC changes between 1999 and 2017 and help to raise the awareness of these changes. Furthermore, the results help to improve future land planning policies for sustainable urban planning.

1.3.2 Individual research objectives

The objectives to for fill the research aim are:

- Implement an object-based change detection method in a GIS workflow.
- Map the LULC in Kalmar with use of multi-temporal satellite images.
- Analyse the LULC changes in the study area between 1999 and 2017.
- Highlight the strengths and weaknesses of using an object-based change detection method to map LULC change.

2.0 Study area, data and software

This chapter describes the study area, data and methodology used in this research. First, the study region is described, followed by the data that is used for mapping the LULC changes. In the last part of this chapter, the software used for this research is described.

2.1 Study area

The study area (Figure 1) is the municipality of Kalmar and is located in the southeastern part of Sweden. The coordinates of the municipality are 56° 40’ 0” N, 16° 22’ 0” E.

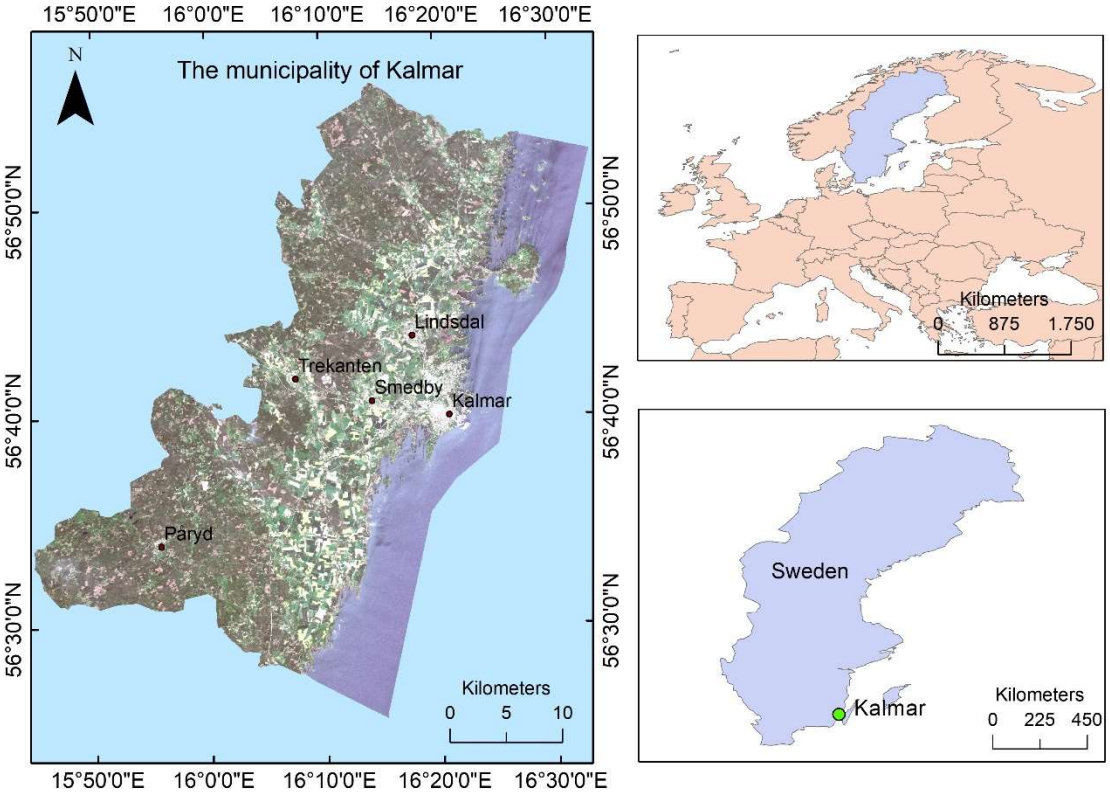

Figure 1: Map with the study area (data: Sentinel 2a ESA and naturalearthdata.com)

The research area has a size of 1,250.96 km^2 from which size 956.9 km^2 consists of land and 294.06 km^2 is water. The municipality has 66.571 inhabitants, divided over 16 localities where Kalmar is the biggest with 35.170 inhabitants (Centralbyrån, 2017).

The study area contains a diversity of land classes, such as urban areas, croplands, pastures, water, forests and other vegetation. Forest and other vegetation are covering the majority of the study area, followed by croplands and pastures. The biggest urban areas are the city of Kalmar with 35.170 inhabitants, followed by the villages of Lindsdal with 5.709 inhabitants and Smedby with 3.607 inhabitants (Centralbyrån, 2017). Most of the agricultural lands are found in the eastern part of the municipality, the western part is dominated by forests for wood production.

2.2 Data

In this study data from various sources is used. The main sources for mapping the LULC changes are Landsat and Sentinel 2a datasets. Landsat and Sentinel 2a satellite imagery has proven to be useful in earth observation studies (Coulter et al., 2016, Immitzer et al., 2016). The used datasets are listed in Table 1.

Table 1: Data sources used for the research.

STUDY DATA						
Data	**Acquisition date**	**Features**	**Resolution**	**Scene size**	**Bands**	**Source**
Landsat 7 ETM+	11 July 1999	Multispectral and Panchromatic	30 m 15 m	170 x 183 km	9	https://earthexplorer.usgs.gov/
Sentinel 2a	27 May 2017	Multispectral	10 m 20 m 60 m	100 x 100 km	12	https://earthexplorer.usgs.gov/

2.2.1 Landsat 7 ETM+

Landsat ETM+ 7 satellite was launched in 1999 by NASA. The device has eight spectral bands and a spatial resolution of 30 meters and a panchromatic band of 15 meters. Each scene is 183 km long by 170 km wide (NASA, 2017).

Figure 2: Subset of the study area Landsat 7 bands 3, 2, 1.

One Landsat image of the 11th of July 1999 (subset is shown in Figure 2), with a cloud cover less than 20%, is freely collected from the website https://earthexplorer.usgs.gov/. Downloaded

data is part of Tier 1 (t1) collection. The satellite data is radiometrically and atmospherically corrected by algorithms. Data is orthorectified and georeferenced into UTM 33 and the World Geodetic System 1984 (USGS, 2017). The collected ETM+ image is from before 2003 and is not disturbed by the failure of the scan line corrector. Technical details of Landsat 7 ETM+ are available in Table 2.

Table 2: Technical details of Landsat 7 ETM+ (USGS, 2017).

Band	Name	Um	Resolution
1	Blue	0.45 – 0.515	30 m
2	Green	0.525 – 0.605	30 m
3	Red	0.63 – 0.69	30 m
4	Near Infrared (NIR	0.775 – 0.90	30 m
5	Shortwave Infrared (SWIR) 1	1.55 – 1.75	30 m
6	Thermal	10.4 – 12.5	60 m
7	Shortwave Infrared (SWIR) 2	2.08 – 2.35	30 m
8	Panchromatic	0.52 – 0.9	15 m

2.2.2 Sentinel – 2a

The Sentinel program consists of multiple satellites from the European Union. The first satellite was launched in April 2014. The Sentinel-2a satellite is launched in June 2015. Applications of the Sentinel 2 satellite are LULC change, water bodies, disaster mapping and vegetation health (ESA, 2017). The repeat circle of the satellite is 10 days. The system has 13 spectral bands, with a resolution of 60, 20 and 10 meters.

Two Sentinel 2a images of 27 May 2017, with a cloud cover less than 20%, were collected from the website https://earthexplorer.usgs.gov/. Downloaded data is part of the 1C collection and radiometrically, atmospherically corrected by algorithms. A subset of the Sentinel 2a data is shown in Figure 3. Furthermore, this data is orthorectified and georeferenced into UTM 33 and

Figure 3: Subset of the study area Sentinel 2a bands 2, 3, 4.

the World Geodetic System 1984 (WGS 84). The footprint of the image is 290 km (ESA, 2017). Technical details of the Sentinel 2a satellite are available in Table 3.

Table 3: Technical characteristics of the Sentinel 2A sensor (ESA, 2017).

Band	Name	Um	Resolution
1	Coastal aerosol	0.443	60 m
2	Blue	0.490	10 m
3	Green	0.560	10 m
4	Red	0.665	10 m
5	Vegetation Red edge	0.705	20 m
6	Vegetation Red edge	0.740	20 m
7	Vegetation Red edge	0.783	20 m
8	NIR	0.842	10 m
8a	Vegetation Red Edge	0.865	20 m
9	Water vapour	0.945	60 m
10	SWIR – Cirrus	1.375	60 m
11	SWIR	1.610	20 m
12	SWIR	2.190	20 m

2.2.3 Reference data

To verify the classified images reference data is used. The research reference data consists of aerial imagery and data from Google Earth. Details of the reference data are listed in Table 4.

Table 4: Reference data used to verify the classification results.

REFERENCE DATA				
Data	**Acquisition date**	**Features**	**Resolution**	**Source**
Aerial photo	1998	Black & White	10 m	Lantmäteriet
Google Earth	2003	Colour	1 m	Digital Globe/Google Earth Pro
Google Earth	19 August 2015	Colour	1 m	Digital Globe/Google Earth Pro

2.3 Software

The segmentation and classification of the satellite images is done with eCognition. eCognition distinguishes itself from other classification software because it classifies images into objects instead of pixels. ArcGIS is used to manage the datasets and to apply some adjustments on the data. Furthermore, this software was used for mapping and analysing the LULC transformations. Excel was used for calculation and statistics.

3.0 Methods

In this chapter, the research methodology is presented. The focus in this chapter is on the following research objective:

- Implement an object-based change detection method in a GIS workflow.

This chapter will first focus on general steps that are needed in object-based change detection. Then the steps that have been taken for object-based change detection for this research are being described and explained.

3.1 General steps of object-based change detection

In general, the process of change detection consists of the following major steps: pre-processing, choosing a change detection technique and accuracy assessment (Lu et al., 2004). Before getting started with detecting changes in LULC, data needs to be pre-processed. Especially data from different aerial or satellites. As sensors have their own characteristics, differences within a study area can appear, which lead to errors and poor change detection results (Lu et al., 2008).

In this study, a post-classification method is applied and therefore the images of 1999 and 2017 are classified separately, before they were used for change detection. To verify the classification result of the satellites images, an accuracy assessment performed. Change detection is then performed by cross-tabulation and overlay-intersection. The workflow is presented in Figure 4.

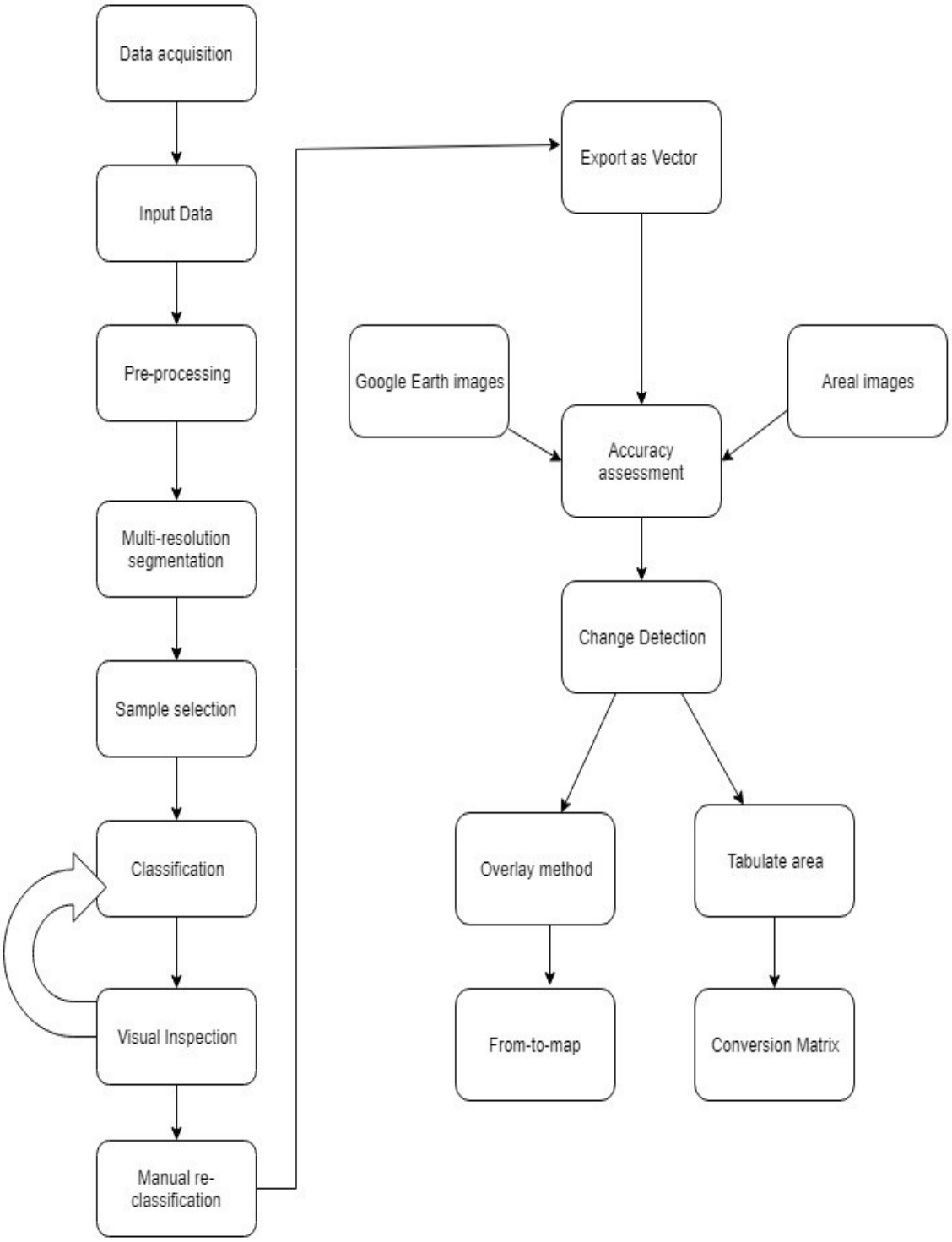

Figure 4: Workflow diagram for the application of an Object-Based Change Detection method for the study area.

3.2 Pre-processing

Remotely sensed data by different sensors can have several errors, which result in miss-alignments, poor classification and change detection results (Lu et al., 2004). Therefore, it is necessary to correct these differences in the pre-processing phase before being applied to other actions regarding change detection. Important steps in pre-processing are atmospheric and radiometric corrections and multi-temporal image registration (Jianya et al., 2008). In this research the following pre-processing steps are described: radiometric correction, georeferencing, geometric correction, image enhancement, merging, bit depth conversion, resampling and raster clipping.

3.2.1 Radiometric correction

Radiometric corrections are necessary when further steps in change detection are applied. Changing radiometric conditions like snow, rain, and sun angles can lead to poor results when LULC change detection is applied without corrections (Paolini et al., 2006). Especially when multi-date satellite images from different sensors for change detection studies are used. With radiometric correction, the effects of a different sun angle, image data, can be minimised (Chen et al., 2005).

In this study radiometric correction is not applied to the datasets, due to several reasons: First, a post-classification change detection is applied and this method reduces the impact of different sensors, changing atmospherical and radiometric conditions (Hussain et al., 2013). Secondly, the acquired datasets are already corrected to some degree. For example, Landsat TM datasets are collected from T1 level (USGS, 2015). This is the highest available data quality and the datasets have undergone standard radiometric calibration. Sentinel 2a datasets have the 1C processing level and are also radiometric and atmospherically corrected (USGS, 2015).

3.2.2 Georeferencing

Often raw satellite images do not have a relation with a geodetic system such as the World Geodetic System 1984 (WGS 84). Before getting started with image processing, the satellite image needs to be georeferenced in a coordinate system that represents real coordinates on the physical surface of the earth. In practice, this means that location information of the raw image is used to connect it to a geodetic system (Hackeloeer et al., 2014). Nowadays there are multiple tools available in GIS software to georeference an image. After georeferencing an image information such as latitude, longitude or UTM coordinates are showed in a GIS-system. In this study images of Landsat 7 ETM+ and Sentinel 2a were already georeferenced into UTM 33 and the World Geodetic System 1984 (WGS 84).

3.2.3 Geometric correction

Remotely sensed images must be geometrically corrected before they can be used for monitoring changes. Often satellites or aeroplanes fly at different heights and this results in image distortions (Jianya et al., 2008). Errors in the geometric registration will lead to errors and poor change detection results. In practice, an error in geometric registration means that two different locations are compared with each other to detect LULC changes (Townshend et al., 1992).

In this study, the Sentinel 2a and Landsat 7 were already geometrically corrected. Before proceeding to the next step, the images were also visually inspected to see if there were no discrepancies in the geometric alignment.

3.2.4 Image enhancement

With image enhancement users can change the digital values of pixels so that the image is easier to interpret with the human eye for visual inspection (Lillesand et al., 1987). For 8-bit images these values are between 0 – 256. Different sensors, atmospheric conditions and land classes result in the fact that the spectral response values of brightness are not the same in every image (Song and Woodcock, 2003). These aspects lead to a difficult interpretation of aerial or satellite images, even when they are already radiometrically corrected. Several techniques for image enhancement are available, but the most common are linear contrast stretch, histogram stretch, standard deviation stretch and a gamma correction (Lillesand et al., 1987). With these techniques, it is possible to adjust the digital values that lay between 0 to 256 for 8-bit images.

In this study, a standard deviation is applied for the Landsat 7 ETM+. The band combination for this dataset was (RGB) 3, 2, 1. This process was done in eCognition software. For the Sentinel 2a image also a standard deviation stretch was applied with band combination 2, 3, 4.

3.2.5 Merge

The dataset of Sentinel 2a consists of two images, because one image was not enough to cover the study area. The whole municipality of Kalmar is covered in a newly merged image.

3.2.6. Bit depth conversion

Sentinel 2a dataset was 16-bits and was converted to 8-bits with the export data tool in ArcMap. This action was needed so that the Sentinel 2a dataset is comparable with the Landsat 7 ETM+ dataset.

3.2.7 Resampling

Sentinel 2a images were resampled from 10 meters to a pixel size of 30 meters, to create the same spatial resolution as the Landsat ETM+ dataset. The images were resampled with the resample tool in ArcMap. For resampling, the nearest neighbour method was used, which is often used for landcover data and classification purposes (Deng et al., 2008, Yuan et al., 2005).

3.2.8 Raster clipping

To decrease the data load and only focus on the municipality of Kalmar the datasets in this study were clipped.

3.3 Image segmentation

In object-based image analysis segmentation is an important step before an analyst can analyse and use the images. Often a proper image segmentation improves the classification result (Blaschke, 2010). Segmentation is the process of grouping pixels from an image into objects (segments) that have the same spectral, pixel and textual values (Hussain et al., 2013). These image segments are used for further analyse processes. There are several segmentation algorithms available. The most common segmentation algorithms provided in eCognition are multiresolution segmentation, quad-tree segmentation, chessboard segmentation, contrast split segmentation, spectral difference segmentation and contrast filter segmentation (eCognition®, 2016).

Image segmentation was performed in this study with the multi-resolution logarithm in eCognition. The multi-resolution logarithm is often used with good results for the segmentation of images (Dingle Robertson and King, 2011, Yan et al., 2006). The algorithm starts at the one-pixel level in an image and works bottom-up based. During the process, more and more pixels are grouped together in larger segments (eCognition®, 2016). Pixels are grouped together if the heterogeneity of the spectral and spatial values does not exceed a minimum (Baatz and Schäpe, 2000). Different parameters can be applied to affect the segmentation result. The value scale parameter is an important threshold for determining how big the segmented object is. A higher scale parameter value results in a bigger group of pixels with spectral similarity (Baatz et al., 2004). Users can define parameters which influence the shape and size of the segment as shown in

Table 5.

Table 5: The parameters in eCognition for the segmentation of pixels in (eCognition®, 2016).

Parameter	Description
Weight of image channels	Adjust the weight for each layer. 1 means full weighting in the process, 0 ignores the layer.
Scale parameter	Adjust the parameter to in- or decrease the size of the segmented object. A low value is a small object, high value increases the size of the object.

Shape	Parameter for defining the weight value for the shape. A low value means a bigger influence for colour.
Compactness	The higher the value, the more compact the object is.
Smoothness	Increasing this value results in smoother objects.

Determining the appropriate parameters for segmentation is often achieved by 'trial and error' and a visual inspection of the segmentation result (Dingle Robertson and King, 2011, Im et al., 2008, Yan et al., 2006).

In this research, the 'trial and error' method with visual inspection was applied. Based on the results for every dataset different segmentation parameters were used. This was because the spectral values of the Landsat ETM+ and Sentinel 2a were not the same. Visual inspection was applied to assess the segmentation results. The segmentation multi-resolution parameters for the Landsat 7 ETM+ and Sentinel 2a dataset are shown in Table 6.

Table 6: Segmentation parameters used for the two datasets in this study.

Parameter	Landsat 7 ETM+	Sentinel 2a
Scale	10	15
Shape	0.5	0.3
Compactness	0.5	0.3

After the segmentation pixels were divided in several objects. In figure 5 is the segmented Sentinel 2a image shown and in figure 6 the segmented Landsat ETM+ image.

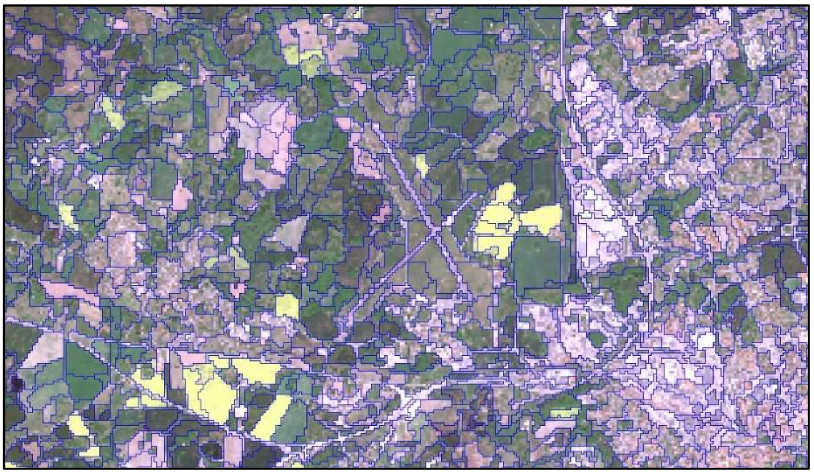

Figure 6: Segmented Sentinel 2a image in eCognition.

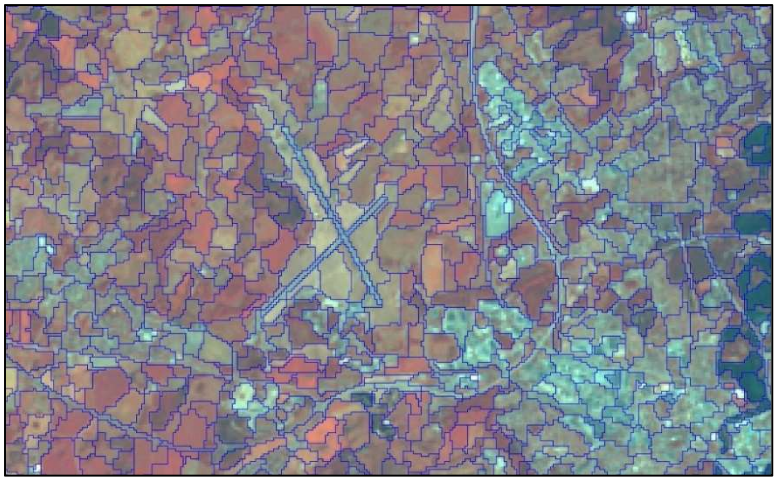

Figure 5: segmented Landsat ETM+ image in eCognition.

3.4 Classification

Classification is about the assigning of objects or pixels to a pre-defined land class. In this study first, the classification scheme was defined. Then a condition was applied and followed by the Standard Nearest Neighbour classifier, provided in eCognition. Additionally, some thresholds were applied to improve the classification performance. The result was visually inspected and if needed wrongly classified objects were manually edited.

3.4.1 Classification scheme

For the assigning of objects to land classes, there are multiple classification schemes available such as the Corine landcover nomenclature (EEA, 2010), and the classification scheme developed by Anderson (1977). Both classification schemes use different levels for the classification of land classes. Land class levels are divided between a general description to a detailed description of a class.

In this study, a detailed classification of LULC classes was not the purpose, since the aim of this research is to map LULC changes between 1999 and 2017. After visual inspection of the Landsat 7 ETM+ and Sentinel 2a images, a modified classification system based on Corine landcover nomenclature was implemented. Furthermore, this classification scheme was developed for European countries and therefore useful in this study area.

The classification scheme in Table 7 shows four classes: agricultural land, vegetation, urban and water.

Table 7: The modified classification scheme (original scheme derived from the European Environment Agency, 2010).

Class	Description	Class name eCognition
Agricultural land	Arable land, permanent crops, pastures	1
Vegetation	Forests, shrub, herbaceous associations, open space with little or no vegetation	2
Urban	Urban fabric, industrial, commercial and transport units, mine dump and construction sites, artificial areas, houses, build structures	3
Water	Inland waters, marine waters	4

3.4.2 Standard nearest neighbour classifier

For classification of the study area the standard nearest neighbour classifier with a fuzzy rule set was used. This classifier is provided in eCognition and is comparable with a supervised classification. The choice to apply the standard nearest neighbour classifier was made based on the users knowledge of the program. The standard nearest neighbour classifier is a supervised classification algorithm. Before the algorithm assigns a class to an object, it calculates the Euclidean distance between a training sample and the object to be classified (Im et al., 2008). The algorithm takes in account several reservations, such as doubts in sensors measurements, mixed pixel problems due to limited resolution and imprecise class descriptions (Im et al., 2008). The classifier assigns a class to an object if it has the same or near identical value with a sample value. Values of the segmented objects are between 0 and 1. The value of 0 represents no identical value with the training sample and the value of 1 represents an identical value, which leads to the assignment of the object (Benz et al., 2004, Im et al., 2008). Before the start of the classification, users derive class samples from the segmented objects. In the classification process, an object is assigned to a class that has the

same or near spectral values as the predefined sample (Yan et al., 2006). The equation of the standard Nearest Neighbour Classifier is:

$$d = \sqrt{\sum \left(\frac{v_f(s) - v_f(o)}{\sigma_f} \right)^2}$$

Whereas:

d = Distance between sample object s and image object o

vf (s) = Feature value of sample object for feature f

vf (o) = Feature value of image object for feature f

σf = Standard deviation of the feature values for feature f

(eCognition®, 2016)

The classification result depends not only on the classification of the image and the usage of training samples, but next to this the quality of the segmentation is important for achieving accurate classification results.

In this study, after the segmentation, the class hierarchy was created in eCogntion with five classes: agricultural lands (1), vegetation (2), urban (3) and water (4) and NoData (5), shown in Figure 7. Then training samples were collected. The collecting of samples (Figure 8) was based on visual inspection of the datasets and the use of aerial images of 1998 and 2015 and Google Earth images.

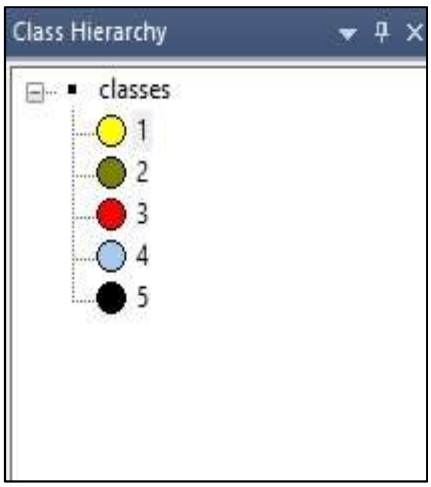

Figure 7: The implemented class hierarchy in eCognition for classification.

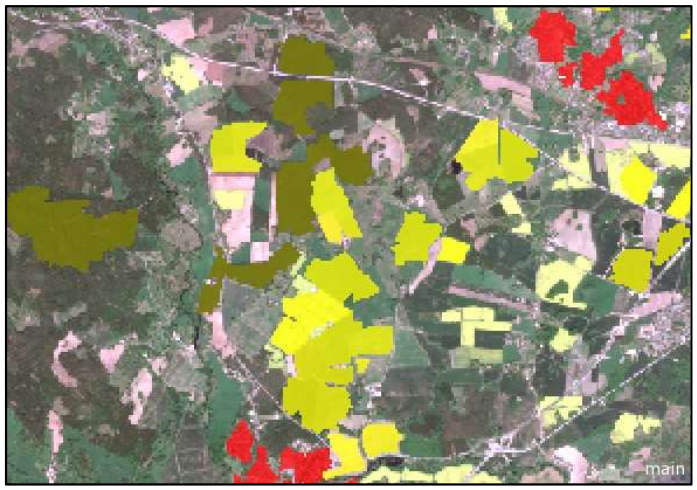

Figure 8: Samples used for classification of the datasets.

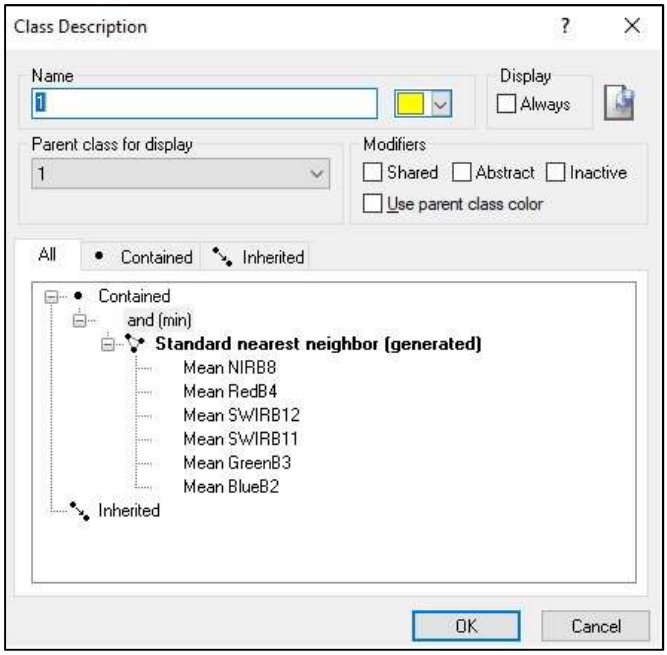

Figure 9: The classification expression used in eCognition for the agricultural lands class.

To classify the image objects with the standard nearest neighbour classifier, the mean values of the Blue, Green, Red, NIR and SWIR bands were used. In Figure 9 the expression is showed for classification of the Agricultural lands.

Thresholds and conditions

To improve the classification, some thresholds and conditions were used during the implementation. For example, the water class was classified with a condition for the Near Infra-Red (NIR) band. The spectral value of water is low in the NIR band (Figure 10). In some

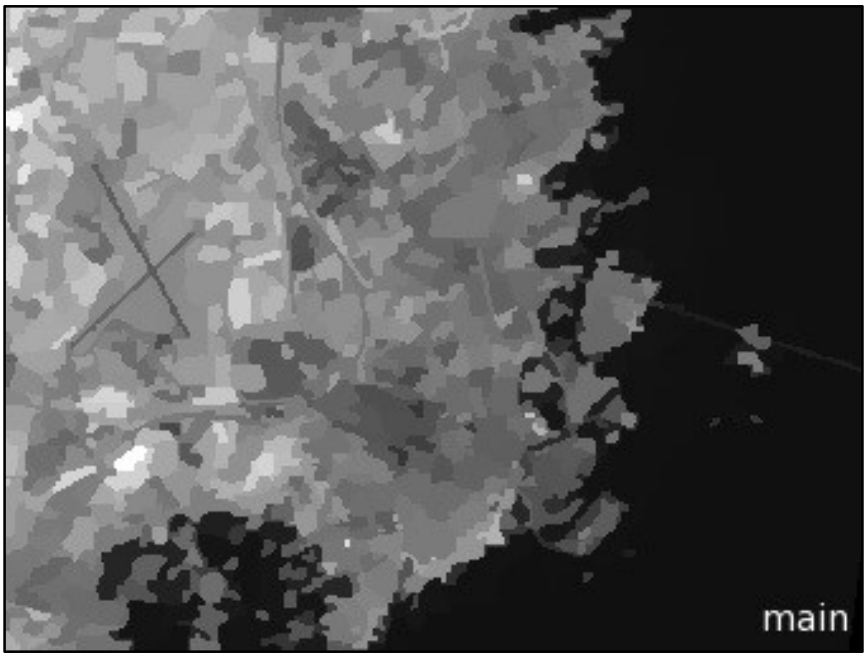

Figure 10: NIR Layer in eCognition. Low NIR values are represented as dark colours.

trial runs, the nearest neighbour classifier had difficulties with the classification of water near the coast of Kalmar. Therefore, a condition was applied to water class.

To improve the classification of the urban class, a Normalized Difference Vegetation Index (NVDI) threshold was applied. The NVDI index is used to distinguish vegetated and non-vegetated areas (Dash et al., 2007). The index implements the spectral values of the Red and NIR bands in an algorithm to calculate vegetation indices. As a result, values between -1 and 1 are shown. The higher the value, the more vegetation is present in the image. The equation to calculate the NDVI is:

$$NDVI = ((NIR - Red) / (NIR + Red))$$

Whereas:

NIR = spectral values Near Infra-Red band

Red = spectral values Red band

(Yuan and Bauer, 2007)

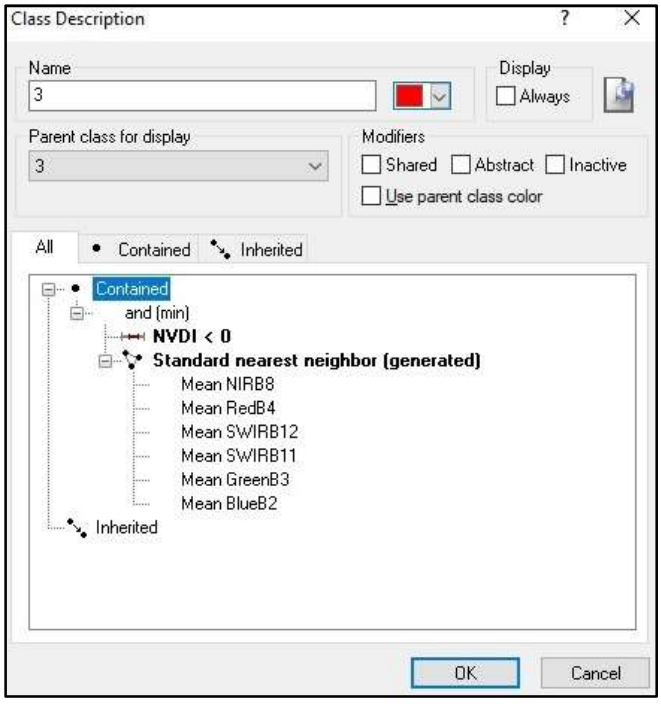

Figure 11: The standard nearest neighbour classifier in eCognition with the NVDI threshold for the classification of the Urban class.

In this study the NDVI index was used as a threshold with the standard nearest neighbour classifier, for a better distinguish between the urban class and the vegetation and agricultural classes (Figure 11). In several studies the NDVI index is used as classifier condition or threshold for classifying (Chuai et al., 2013, Dash et al., 2007).

After a classification cycle, the image was inspected on errors. Misclassifications were adjusted with extra training samples, and the classification cycle was repeated. Then the image was visually inspected, and misclassifications were manually edited.

The merge tool was applied to improve performance later in ArcMap. The whole ruleset is shown in Figure 12. After classifying the images, the results were exported as a vector polygon layer to ArcMap.

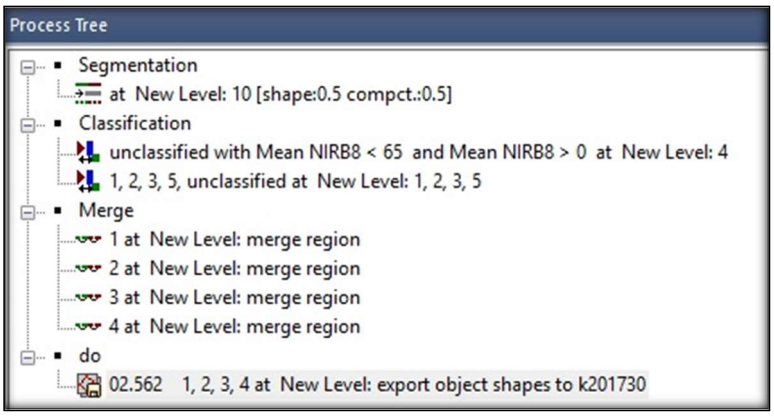

Figure 12: The workflow for the classification of the datasets in eCognition.

3.5 Accuracy assessment

Accuracy assessment is about the verification of the classified data and is an important part of the workflow in LULC change detection. With an accuracy assessment, the quality of the classification is determined. To observe the LULC changes in the study area the classification results of the datasets must be verified (Stehman and Czaplewski, 1998). In a classification process several errors can occur that can lead to insufficient results. Errors can occur from incorrect image registration, wrong interpretation of a class due to coarse resolution or insufficient training samples (Lu and Weng, 2007).

There are several options to perform an accuracy assessment. The error matrix is a well-known method and is used in multiple LULC change detection studies (Congalton and Green, 2008). An error matrix contains the following elements: (a) Ground data collection, (b) Classification scheme, (c) Sampling scheme, (d) Spatial auto correlation, (e) Sample size and sample unit. Elements such as Kappa coefficient, overall accuracy, omission and commission error complement the error matrix (Congalton and Plourde, 2002).

Ground control points (GCPs) are collected from reference data or field visits to compare the classified data with the data from the GCPs. The collected data is then compared with the classified data in the error matrix.

To verify the classification results for the images of 1999 and 2017, in this study an error matrix was implemented to calculate the classification accuracy per class. With the input of the error matrix, the Kappa coefficient and the user and producer accuracy could be derived.

To assess how the classification results performed, ground control points were deployed with the creating random points tool from software Geospatial Modelling Environment. Several authors suggest using 50 ground control points samples for each class (Congalton and Plourde, 2002). Since there are four classes in this study, this leads to a total of 200 ground control points. A stratified sampling method was applied to ensure that 50 samples were distributed in each class.

Google Earth images and aerial photos were used as reference data to check if the classification was appropriate. Google Earth images were from 2003 and 2015, areal images were from 1998 and 2016. For the classified Landsat ETM+ image of 1999, areal images from 1998 and Google Earth images of 2003 were used. The high-resolution images of Google Earth from 2003 were not covering the whole study area. Therefore, additionally areal images from 1998 with a resolution of 10 meters were used for the accuracy assessment of the classified image from 1999.

Several studies have proven that Google Earth images can be used to verify the accuracy of classified images (Knorn et al., 2009, Kuemmerle et al., 2009). Because this research contains only four land classes, no GPS ground control points from field visits were collected.

Figure 13: Subset of study area in Google Earth with the ground control points to compare classified results with the aerial data.

First 50 stratified sample points per class were distributed in the study area. Then the distributed points were converted in ArcMap into a KMZ file and opened in Google Earth (Figure 13). The classified class was then verified in Google Earth and in ArcMap against the areal reference data from 1998 or 2016.

3.6 Change detection

With change detection the purpose is to discover changes between two or more multidate images. As stated before, there are multiple change detection techniques developed but none of them is suitable for every purpose. Choosing an appropriate change detection technique depends on the objectives of the study and the characteristics of the study area.

3.6.1 Post-classification change detection

In this research, an object-based post-classification change detection method was applied. First, with this method it is possible to minimise the atmospheric effects and differences between the sensors of Landsat 7 ETM+ and Sentinel 2a. Secondly, the post-classification method generates a conversion matrix. With this matrix it is possible to see the transformation from one class into another (Shalaby and Tateishi, 2007). Furthermore, this classification method is often used in change detection studies (Hussain et al., 2013). However, the change detection accuracy is highly depended on the accuracy of the classified images, since poor classification leads to inaccurate change detection results (Lu et al., 2004).

In this study, and after classification in eCogntion, the images of 1999 and 2017 were exported as a thematic vector shapefile in ArcMap. LULC Statistics for the classified maps were calculated separately. Then the percentage of LULC changes is calculated by the following equation:

Percentage LULC change = (Area final year – Area initial year)/ (Area initial year) * 100.

The overlay-intersection method was used to detect changes between the classified images of 1999 and 2017. This method revealed ‘from-to’ changes of land classes. A from-to map was created to visualize the LULC changes. The focus in this study is on change from the vegetation and agricultural lands into urban areas. Also, a change threshold of > 0.1 square kilometres was used to delete sliver polygons and wrong detected changes. In the last step the tabulate area tool was applied in ArcMap to calculate the change in square kilometres between the classes.

4.0 Results

In this chapter the results the study are described an presented. The focus in this chapter is on the following research objectives:

- Map the LULC in Kalmar with use of multi-temporal satellite images.
- Analyse the LULC changes in the study area between 1999 and 2017.

First, the results of the object-based classification will be described, including classification accuracy, map statistics and thematic maps of LULC for the study dates. Secondly, the results of the post-classification object-based change detection method will be described and visualized, including drivers for the LULC transformation between 1999 and 2017.

4.1 Accuracy assessment

4.1.1 Landsat 7 ETM+ 1999

The classification result of the Landsat ETM+ image achieved satisfying accuracy results (Table 8). The overall accuracy of the Landsat image is 95% with a Kappa index of 93%. The four classes have an individual users accuracy between 88% and 100%.

Table 8: Error matrix with for the Landsat ETM+ dataset with classification results.

Landsat 7 ETM+ 1999	**Reference data**				**Classification Accuracy**	
LULC classes	**Agriculture**	**Vegetation**	**Urban**	**Water**	**Producers accuracy**	**Users accuracy**
Agricultural lands	45	4	1	0	90%	88%
Vegetation	2	48	0	0	92%	96%
Urban	4	0	46	0	98%	92%
Water	0	0	0	50	100%	100%
Overall accuracy					**95%**	
Kappa Index					**93%**	

The lowest accuracy was in the agricultural lands class with a producers accuracy of 90% and a users accuracy of 88%. Water was the class with the highest accuracy with a score of 100% for both the producers and users accuracy. The error matrix shows that in the agricultural lands class the most errors were made with vegetated areas. Also, in the urban class, there were misclassifications with the agricultural land class.

4.1.2 Sentinel 2a 2017

The Sentinel image of 2017 had an overall accuracy of 95% and a Kappa statistic of 93%. The individual producers and users accuracies of the four classes ranged between 90% and 100%. The error matrix with and the accuracy results are shown in Table 9.

Table 9: Error matrix with for the Sentinel 2a dataset with classification results.

Sentinel 2a 2017	**Reference data**				**Classification Accuracy**	
LULC classes	**Agriculture**	**vegetation**	**Urban**	**Water**	**Producers accuracy**	**Users accuracy**
Agricultural lands	46	4	0	0	90%	92%
Vegetation	3	45	2	0	92%	90%
Urban	2	0	48	0	96%	96%
Water	0	0	0	50	100%	100%
Overall accuracy					**95%**	
Kappa Index					**93%**	

The lowest accuracy in the classified images of 2017 was in the agricultural lands and vegetation class. Agricultural lands had a producers accuracy of 90% and a users accuracy of 92%. The vegetation class had a producers accuracy of 92% and a users accuracy of 90%. In this map, the users accuracy of the classification of agricultural lands was higher compared to the classified map of 1999. The urban class achieved a high score of 96% for the producers and users accuracy. Water was again the class with the highest accuracy with a score of 100% for both the producers and users accuracy. The error matrix for 2017 shows that in the agricultural lands class the most errors were made again with vegetated areas. Also, in the urban class there were misclassifications with the agricultural land class.

4.2 Classification and map statistics

LULC maps 1999 and 2017 are shown in Figure 14 and Figure 15. Map statistics (Table 10) for 1999 revealed that vegetation covers the biggest area in the study area with 695 km^2 (55.20%). The second major class is water with 298 km^2 (23.66%), followed by agricultural lands with 231 km^2 (18.34%) and urban 35 km^2 (2.77%).

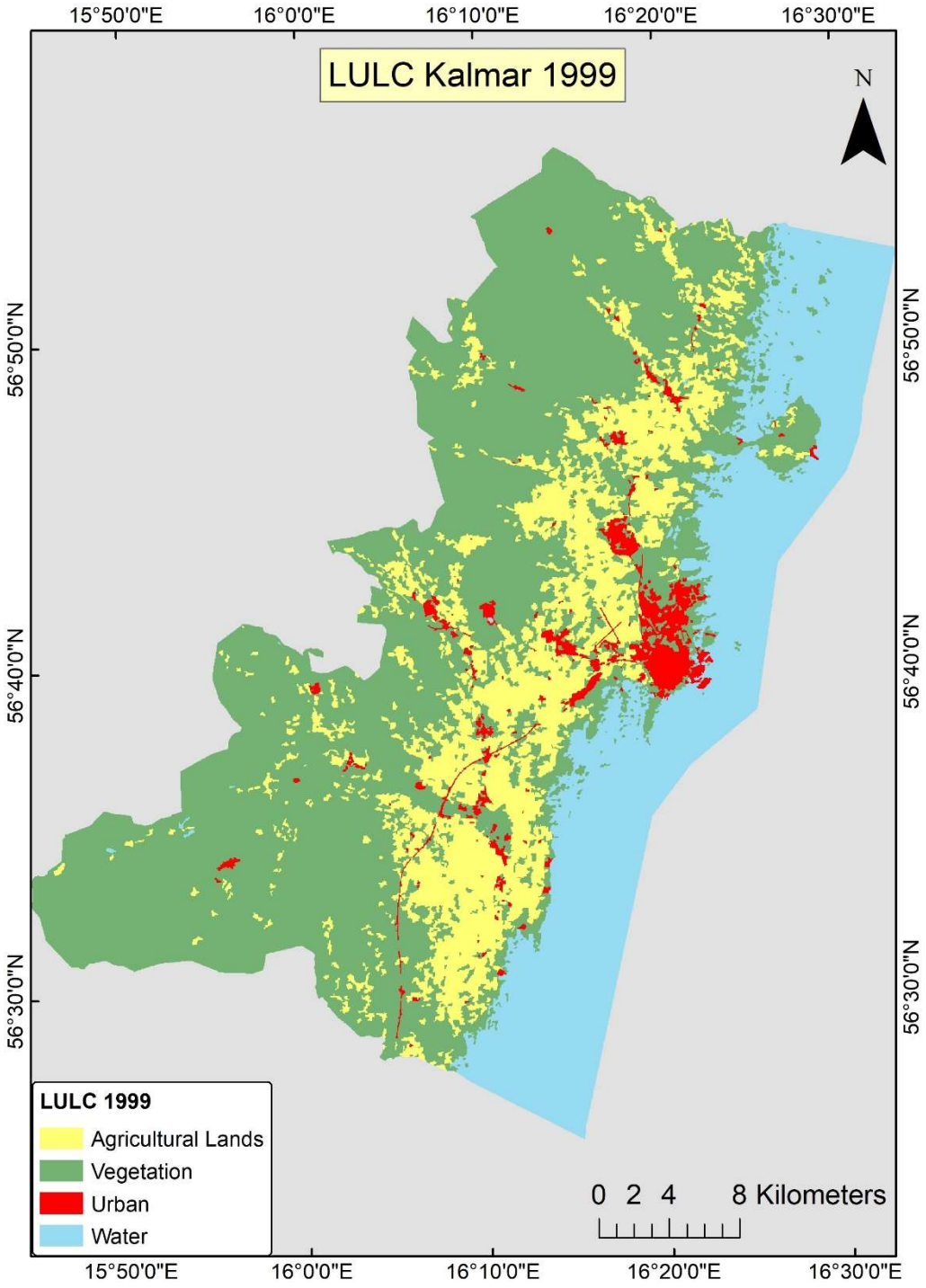

Figure 14: Land use and land cover in the municipality of Kalmar in 1999.

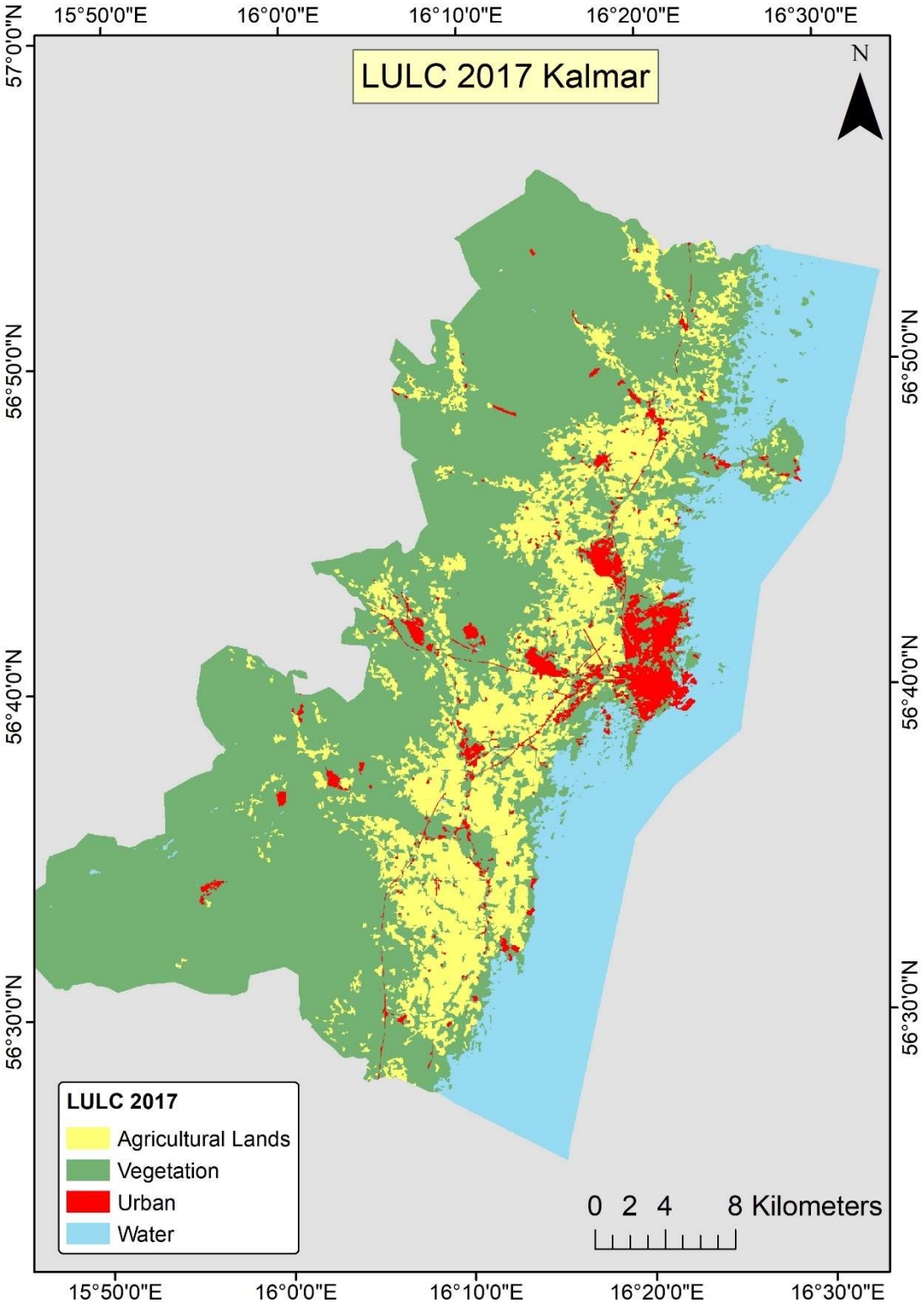

Figure 15: Land use and land cover in the municipality of Kalmar in 2017.

In 2017 vegetation is still the biggest land class with 713 km^2 (56,63%), followed by the water class with 299 km^2 (23,74%). Agricultural lands covered the area with 207 km^2 (16,44%) and urban areas covered around 42 km^2 (3,33%) in 2017.

Table 10: Map statistics for the classified images.

Land use/cover categories	1999		2017	
	Km^2	**Percentage**	**Km^2**	**Percentage**
Agricultural lands	231	18.34	207	16.44
Vegetation	695	55.20	713	56.63
Urban	35	2.77	42	3.33
Water	298	23.66	299	23.74
Total	1259	100	1259	100

Comparing the statistics of 1999 and 2017 reveals that there is a decline in agricultural lands. An increase is visible in the classes vegetation, urban and water. Vegetation increased from 695 km^2 to 713 km^2, urban class increased also from 35 km^2 to 42 km^2. Water stayed stable with only a small increase from 298 km^2 to 299 km^2. The classification shows a decrease of agricultural lands from 231 km^2 in 1999 to 207 km^2 in 2017.

Table 11: LULC changes between 1999 and 2017.

Change in LULC between 1999 and 2017		
Class	**%**	**Km^2**
Agricultural lands	-10.38	-24
Vegetation	2.58	18
Urban	20	7
Water	0.33	1

Post-classification comparison of the two classified (Table 11) images shows significant LULC changes in the study area. This study shows a decrease of agricultural lands containing a loss of 24 km^2 (-10.38%) between 1999 and 2017. Urban areas expanded with 7 km^2 (20%) and the vegetation class expanded with 18 km^2 (2.58%). The water class did not increase significantly (1 km^2, 0.33%).

4.3 Change Detection

4.3.1 change detection statistics

The cross-tabulation matrix in Table 12 provides insight in the changes between the classes. The total study area is 1258,08 km^2. Between 1999 and 2017 around 1123,75 km^2 did not change, the remainder of 134,38 km^2 converted in other classes.

Table 12: From-to changes between 1999 and 2017 in km^2.

From-to changes in km^2						
	1999					
2017	**LULC-classes**	**Agricultural lands**	**Vegetation**	**Urban**	**Water**	**Total**
	Agricultural lands	165,55	39,02	2,88	0,03	206,49
	Vegetation	59,88	640,72	6,92	4,37	711,89
	Urban	6,51	10,14	25,02	0,43	42,10
	Water	0,08	3,92	0,14	293,46	297,59
	Total	231,02	693,81	34,96	298,29	

The nature of changes revealed that major changes occurred between the agricultural and vegetation class. For instance, 231,02 km^2 of agricultural land covered the area in 1999 and 206,49 km^2 in 2017. Out of 231,02 km^2 that was agricultural land in 1999, 165,55 km^2 was still in 2017 but 59,88 km^2 was transformed in vegetation, 6,51 km^2 converted into urban areas and 0,08 km^2 into water.

The vegetation class covered the study area with 693,81 km^2 in 1999 and 711,89 km^2 in 2017. Out of the vegetation class 640,72 km^2 was still vegetation in 2017 but 39,02 km^2 was transformed into agricultural lands class, 10,14 km^2 was converted into urban areas and 3,92 km^2 into the water class.

The urban class was covering the study area with 34,96 km^2 in 1999 and 42,10 km^2 in 2017. Around 25 km^2 was still urban in 2017 but 2,88 km^2 was converted into the agricultural class, 6,92 km^2 was converted into vegetation and 0,14 km^2 transformed into the water class.

In the water class the smallest transformations took place. Water was covering the study area with 298,29 km^2 in 1999 and 297,59 km^2 in 2017. Out of the water class 293,46 km^2 was still water in 2017 but 0,03 km^2 was converted in agricultural lands, 4,37 km^2 converted into vegetation and 0,43 km^2 converted into the urban class.

In Table 13 are the change percentages shown between the classes. In percentages the biggest transformation changes occurred in the agricultural land class and the urban class. The third biggest change was in the vegetation class. In the water class the smallest change in percentage occurred between 1999 and 2017.

Table 13: From-to changes between 1999 and 2017 in percentages.

From to changes in percentages					
	2017				
1999	**LULCclasses**	Agricultural lands	Vegetation	Urban	Water
	Agricultural lands	71,19	25,91	2,82	0,03
	Vegetation	5,62	92,22	1,46	0,56
	Urban	8,25	19,78	71,57	0,39
	Water	0,01	1,46	0,14	98,34

4.3.2 change detection maps

Figure 16 shows the LULC types and the from vegetation or agricultural lands that changed into urban areas between 1999 and 2017. To visualize the LULC changes and to delete false transformations a threshold of > 0.1 km^2 was applied. Most of the changes occurred near the edges of villages and the city of Kalmar. An image of the whole map is shown in appendix A.

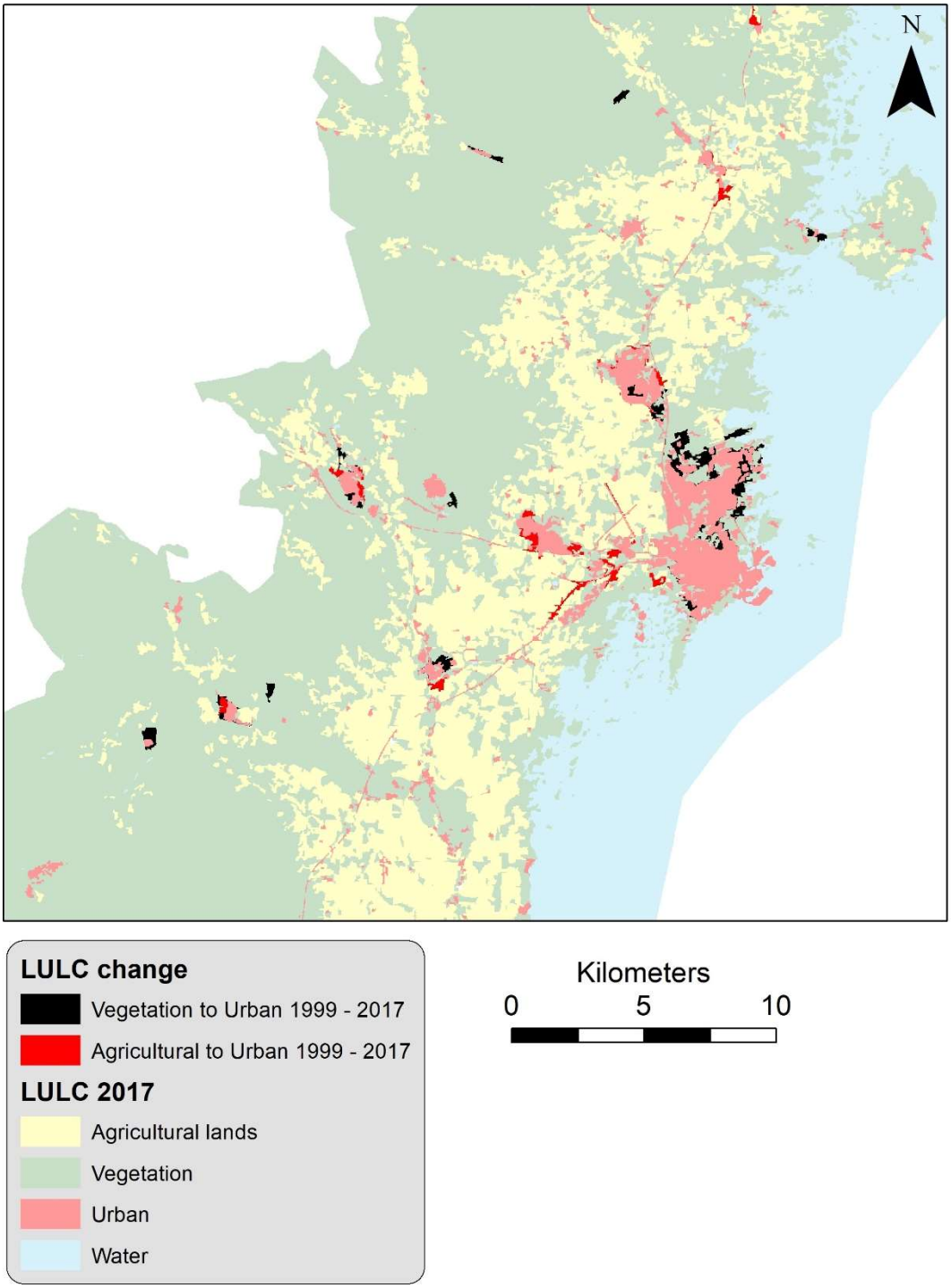

Figure 16: Subset of study area with LULC transformations into urban areas between 1999 and 2017.

Figure 17 shows a subset of the 'from-to' change map but more zoomed in around the biggest urban areas: Kalmar, Lindsdal and Smedby. In the northern part of the city of Kalmar, urban areas expanded between 1999 and 2017. Mostly vegetated areas were converted into urban classes. In the southwestern part of Kalmar agricultural lands were lost and converted in urban parts. Near the village of Smedby the mainly agricultural lands were converted. In general, most expansions took place at the edges of the villages and the city.

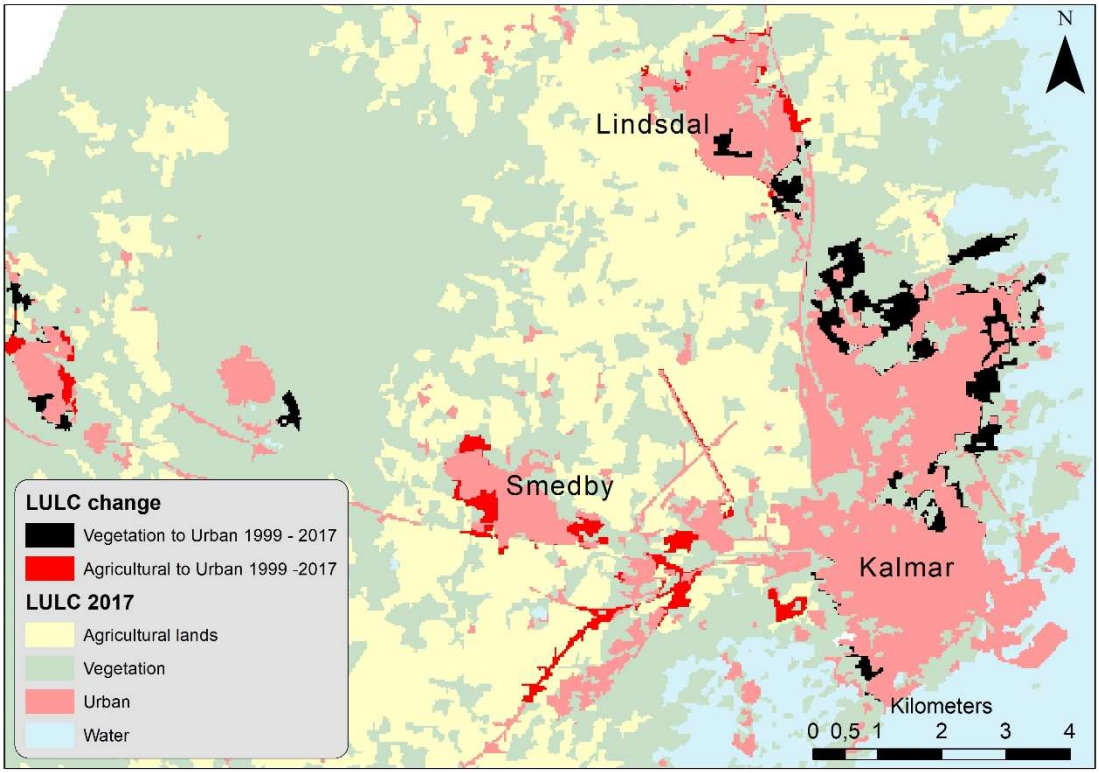

Figure 17: Subset of LULC changes near Kalmar, Smedby and Lindsdal.

Also, clearly visible is the extension of the highway E22 (Figure 18). This highway is extended between 1999 and 2017. The figures (Figure 20 and Figure 19) below from Google Earth are also showing this LULC transformation.

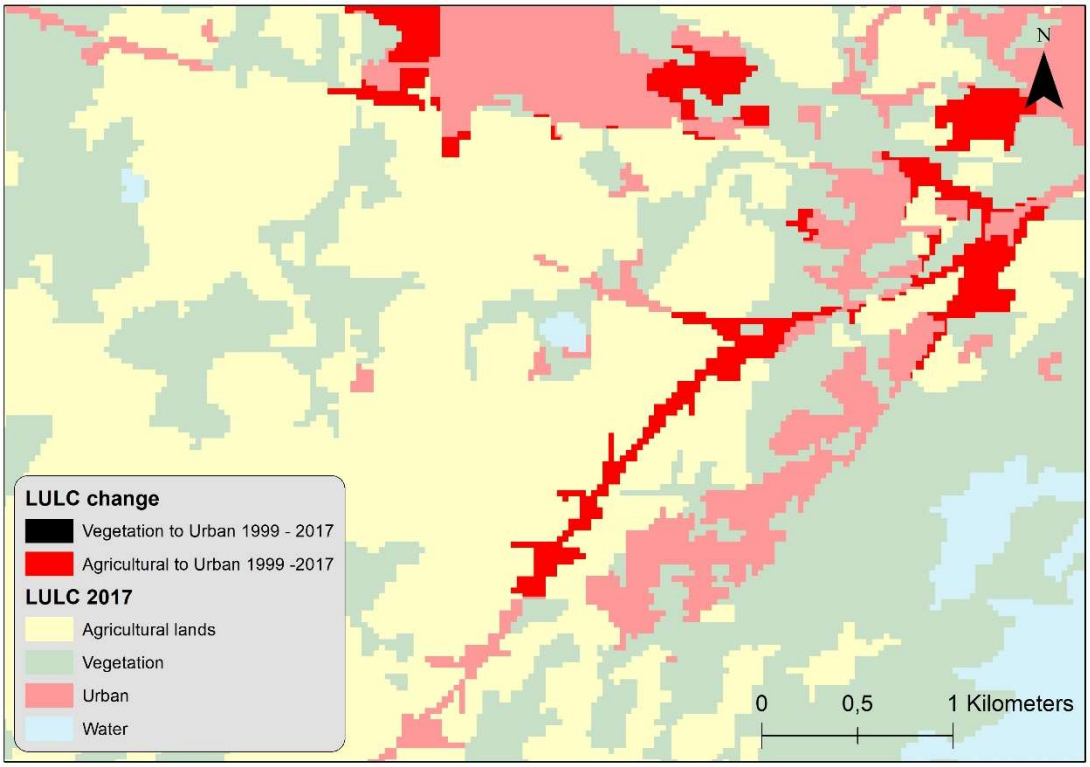

Figure 18: Subset of study area that shows the extension of highway E22.

Figure 20: Google Earth image of 2003 without the extended highway E22.

Figure 19: Google Earth image of 2016 with the extended highway E22.

5.0 Discussion

In this chapter the research results will be discussed, and the focus will be on the following research objective:

- Highlight the strengths and weaknesses of using an object-based change detection method to map LULC change.

The strengths of the object-based change detection method will be discussed, followed by the weak points of this method.

5.1 Strengths of using an object-based classification and change detection

The object-based classification of the Landsat 7 ETM+ and the Sentinel 2a images with a spatial resolution of 30 meters for 1999 and 2017 was successful. In this research, the overall accuracies of both images were 95% and per class accuracy is between 90% and 100%. Kappa index was for the Landsat 7 ETM+ and Sentinel 2a image 93%. Minimum thresholds for the overall accuracy set at 85% by Andersson (1977). For the individual classes the minimum is set at 70% (Thomlinson et al., 1999). Thus object-based classification with the standard nearest neighbour classifier combined with visual inspection and manual classification was accurate.

Post-classification change detection between 1999 and 2017 showed a decrease in agricultural lands. This trend is also visible in other parts of Sweden and in Europe (Kasanko et al., 2006, Wästfelt and Zhang, 2016). However, drivers for the loss of agricultural lands were not only due to urbanization. The expansion of vegetated areas was also a part of this decrease in agricultural lands. The loss of farmlands caused by the increase of vegetated areas was probably caused by the expansion of forestries in the study area.

The 'from-to' map was reduced to show only the 'vegetation to urban' and 'agricultural lands to urban' changes. It was assumed that other changes such as 'urban to vegetation' and 'urban to agricultural lands' were unlikely. A threshold was applied of 0.1 km^2 to reduce the amount of false change detection errors. Every change below 0.1 km^2 was handled as 'no-change'. The change detection map showed that near the city and village edges often land was converted into urban areas. The change detection techniques showed that it can locate areas were LULC conversions took place in the study area. The map also showed the areas were no changes occurred between 1999 and 2017.

For segmentation of the images a multi-resolution segmentation algorithm was used for grouping the pixels into heterogeneous groups. Appropriate segmentation parameters were

found by trial and error as suggested by Hussain at all (2013). After segmentation a visual inspection was needed to analyse the result. Finding the right parameters differs for each sensor. Furthermore, different thresholds were used, but there was no quick solution that improved the result.

In general: Applying the standard nearest neighbour method with visual inspection and manual classification for classifying the images was useful in this research. However, in this study, there were difficulties in classifying agricultural lands versus vegetation. For example, the classifier often classified woodlands (vegetation class) into the agricultural class. To solve this problem different vegetation indices (e.g. NVDI) and thresholds were used (e.g. rectangular fit) but these did not improve the classification results.

5.2 Problems of the study

The change detection method with the overlay method was not without errors. Some values in the change-matrix are not realistic. For example, it is unlikely that 6,92 km^2 from urban areas are converted into vegetation as shown in Table 12. Also, the conversion from urban areas into agricultural lands (2,88 km^2) between 1999 and 2017 is unrealistic. As stated before and by other researchers (Lu et al., 2004) the accuracy depends on the classified images. If a class is wrongly classified, this will result in a false change error. Despite high classification accuracies, there were several false changes errors that were caused by misclassifications. In Figure 21 is the unmodified 'from-to' map shown for the study area. The map shows many small and false change detection errors. A bigger size of the 'from-to map' for the study area is available in appendix B.

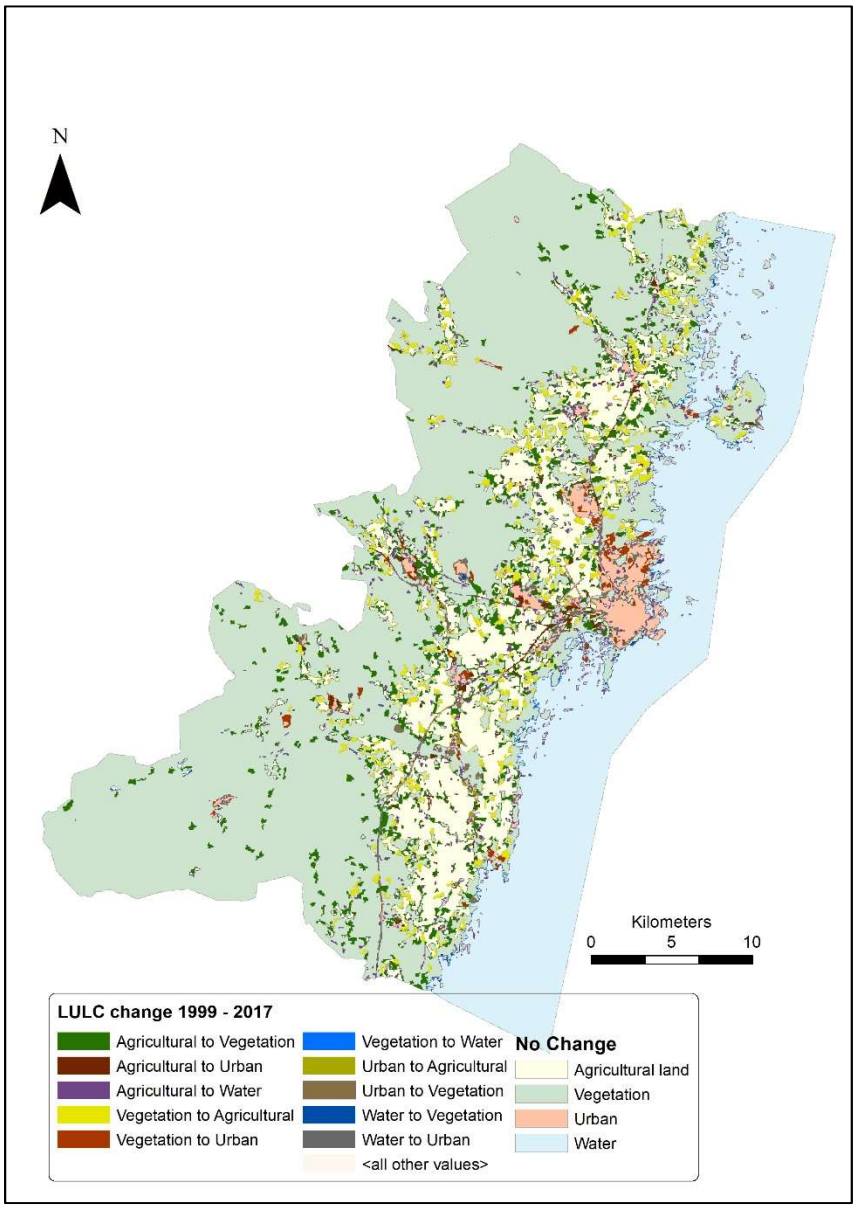

Figure 21: Unmodified map of LULC change between 1999 and 2017.

The object-based change detection approach in the study area led to several sliver polygons. In Figure 22 a subset of the study area is shown with several sliver polygons. These polygons resulted in false change detection errors. Near the edges of the land classes, these false change detection errors are visible. These sliver polygons are a result of overlapping the classified images of 1999 and 2017. Chen et al. (2012) stated that this problem arises when different segmentation parameters are used. To reduce the impact of this problem, in this study a threshold was applied of > 0.1. Changes below this threshold were ignored. The downside of this approach is that also correct change detection information is lost. Despite some practical solutions more research is still needed to overcome the problem of sliver polygons (Tewkesbury et al., 2015).

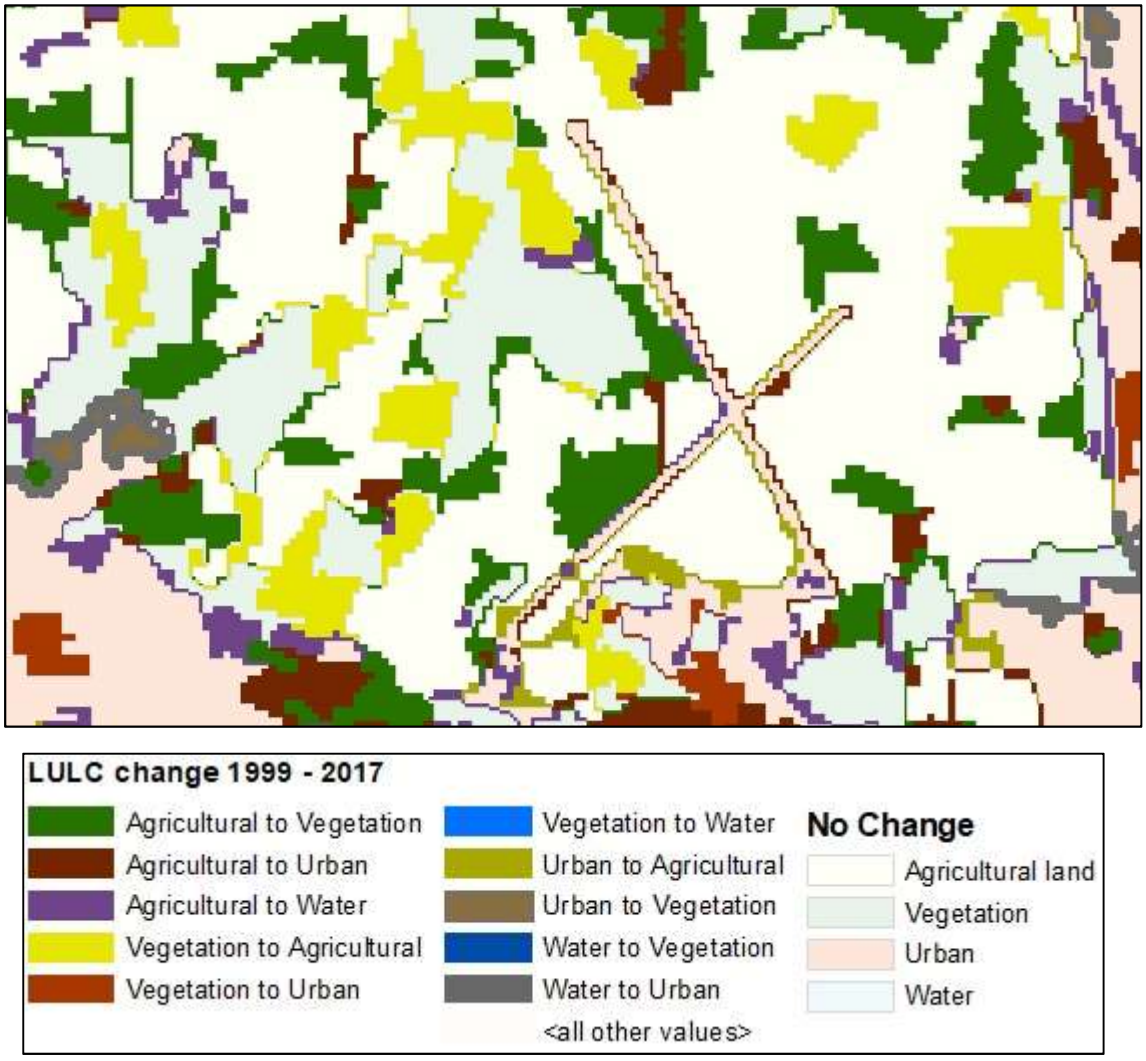

Figure 22: Subset study area with sliver polygons at the edges of land classes.

Some misclassifications were caused by the use of medium resolution images. In this study the pixel-size was 30 meters and segmented objects could represent multiple classes. This is because the used pixel size used was bigger than some geographical objects. As a result, there were several false change detection errors. Chen et all (2012) suggested to use high-resolution images to solve this problem and to create a more stable comparison between two classified images. In this study, medium resolution images were used since high-resolution images were not freely available.

There were also problems with the classification between agricultural lands and urban areas. Especially if the agricultural lands were related to crop, these grounds were often classified as urban areas. Probably this has to do with the fact that the classifier has difficulties with the spectral signature between these areas and the heterogeneity in urban and agricultural areas (Zhang et al., 2014).

A limitation in this study is that the change detection map has no accuracy assessment. Therefore, it is not possible to assess the quality of the LULC change map. However, literature shows that applying an accuracy assessment on the change detection result is not always applied (Kindu et al., 2013, Rawat et al., 2013). In this study the accuracy assessment for the change detection result was not applied due to the time limit.

6.0 Conclusion

The aim of this study was to use an object-based change detection method to map and LULC change in the municipality of Kalmar. The specific research objectives related to this research were to:

1. Implement an object-based change detection method in a GIS workflow.
2. Map the LULC in Kalmar with use of multi-temporal satellite images.
3. Analyse the LULC changes in the study area between 1999 and 2017.
4. Highlight the strengths and weaknesses of using an object-based change detection method to map LULC change.

This chapter will revisit the research objectives, summarize the findings and conclude this research work. In the last part, recommendations for future research will be described.

6.1 Research objectives, summary of findings and conclusions

6.1.1 Objective 1: Implement object-based change detection method in a GIS workflow.

In this study, a post-classification change detection technique was applied to avoid the impact of different sensors, atmospheric influences on the classification and change detection results. Furthermore, with the post-classification method it is possible to show the 'from-to' changes of land classes. Two satellite images of 1999 and 2017 were collected and pre-processing of the data was done in ArcMap. Images were segmented in geographical objects and classified in four classes with the eCognition software. Then the classified images were exported as vector layer into ArcMap. The accuracy of the classified images was checked with an accuracy assessment based on reference images. To detect changes and to discover 'from-to' changes the overlay and tabulate method was applied in ArcMap.

The main conclusion that can be drawn when implementing an object-based change detection method in a GIS-workflow, is that there is no perfect fit for every case. The application of this method depends in several stages of the workflow on trial and error and every satellite image has its own influence on the segmentation and classification results. Many parameters can be applied to adjust the result, but much depends on the skills of the research analyst.

6.1.2 Objective 2: Map the LULC in Kalmar with use of multi-temporal satellite images.

The LULC of the municipality was mapped for the years of 1999 and 2017. The two classified maps show the distribution of land classes. The overall accuracies for both maps were 95% and the Kappa index was 93%. Map statistics show that in the map of 1999 vegetation is the

biggest class in the study region followed by water, agricultural lands and urban. This distribution order is the same for the classified image of 2017.

The main conclusion that can be drawn is that -with an object-based classification of two medium resolution images- it is possible to achieve high classification accuracies. Furthermore, this method has proven to be very useful to map and gain insight in the LULC distribution at a local scale for different years.

6.1.3 Objective 3: Analyse the LULC changes in the study area between 1999 and 2017.

Object-based post-classification change detection method revealed several LULC transformations in the study area. Agricultural lands decreased between 1999 and 2017 from 231 km^2 to 207 km^2 (-10.38%). Urban areas expanded significantly from 35 km^2 to 42 km^2 (20%). Vegetation increased from 695 km^2 to 713 km^2 (2.58%). 'From-to tables' showed the drivers for the LULC changes. Urbanization in the study area was responsible for the conversion of agricultural lands and vegetation areas. Besides that, the expansion in vegetated areas was also responsible for a decrease in farmlands. The 'from-to map' provided insight where the urban expansion occurred in the study area.

The conclusion that can be drawn for this objective is that agricultural land decreased in the study area and that the urban expansion is for a part responsible for this decline. This trend is also visible at a national and worldwide scale.

6.1.4 Objective 4: Highlight the strengths and weaknesses of using an object-based change detection method to map

The object-based classification of the Landsat 7 ETM+ and the Sentinel 2a images was successful. Overall accuracies of both images were 95% and per class producers accuracy is between 90% and 100%.

Post-classification change detection revealed map statistics that showed the changing size of LULC classes between 1999 and 2017. Another advantage of this method was the discovery of the drivers for LULC transformations. A downside of this method is that the change detection results contained several errors. Often the results contained false change detection errors that were caused by misclassifications. The amount square kilometres in the conversion table (Table 12) is therefore overestimated and some transformations such as urban to vegetation are unrealistic. More research is needed to overcome the problem of sliver polygons, when classified images are combined. Object-based post-classification change detection derives insights in a changing landscape and what caused these changes. This information can help to

develop better planning policies for a sustainable land management. However, analysts must realize that the method is not faultless, and classifications of satellite images must be of high accuracy.

6.2 Recommendations for future research

Future research for this study area should be carried out with high-resolution images. For example, Sentinel 2a data has a spatial resolution of 10 meters and is freely available. This satellite is available since 2016. With high-resolution images, it is possible to map the LULC changes more accurately and to analyse the LULC transformations more precisely.

Despite the standard Nearest Neighbour Classifier in eCognition worked well for this study area with four land classes, future research should be concentrated in developing a more robust ruleset for classifying remotely sensed images. Especially for study areas with a mix of agricultural and vegetated areas and with medium (30m) resolution images. Focus can be on developing a segmentation method that is not based on trial and error which can save time for the analyst.

To decrease the false change detection errors future research should focus on a segmentation method that reduces the differences between the shape and size of segmented objects of two multi-date images. This can help to increase the accuracy of a post-classification change detection method.

It is also recommended to map and analyse LULC changes for other parts of Sweden, to investigate if the trend of decreasing agricultural lands and increasing urban areas is also happening in other regions. More LULC change studies can help to face challenges like the declining agricultural lands in combination with growing population in a better way. With as result more sustainable regional and local planning policies.

References

ABD EL-KAWY, O. R., RØD, J. K., ISMAIL, H. A. & SULIMAN, A. S. 2011. Land use and land cover change detection in the western Nile delta of Egypt using remote sensing data. *Applied Geography,* 31**,** 483-494.

AN, K., ZHANG, J. & XIAO, Y. 2007. Object-oriented urban dynamic monitoring — A case study of Haidian District of Beijing. *Chinese Geographical Science,* 17**,** 236-242.

ANDERSON, J. 1977. Land use and land cover changes. A framework for monitoring. *Journal of Research by the Geological Survey,* 5**,** 143-153.

ANTROP, M. 2004. Landscape change and the urbanization process in Europe. *Landscape and urban planning,* 67**,** 9-26.

BAATZ, M., BENZ, U., DEHGHANI, S., HEYNEN, M., HÖLTJE, A., HOFMANN, P., LINGENFELDER, I., MIMLER, M., SOHLBACH, M. & WEBER, M. 2004. eCognition professional user guide 4. *Definiens Imaging, Munich*.

BAATZ, M. & SCHÄPE, A. 2000. Multiresolution segmentation: an optimization approach for high quality multi-scale image segmentation. *Angewandte geographische informationsverarbeitung***,** 12-23.

BENZ, U. C., HOFMANN, P., WILLHAUCK, G., LINGENFELDER, I. & HEYNEN, M. 2004. Multi-resolution, object-oriented fuzzy analysis of remote sensing data for GIS-ready information. *ISPRS Journal of Photogrammetry and Remote Sensing,* 58**,** 239-258.

BLASCHKE, T. 2010. Object based image analysis for remote sensing. *ISPRS Journal of Photogrammetry and Remote Sensing,* 65**,** 2-16.

BLASCHKE, T., LANG, S., LORUP, E., STROBL, J. & ZEIL, P. 2000. Object-oriented image processing in an integrated GIS/remote sensing environment and perspectives for environmental applications. *Environmental information for planning, politics and the public,* 2**,** 555-570.

BRANNSTROM, C., JEPSON, W., FILIPPI, A. M., REDO, D., XU, Z. W. & GANESH, S. 2008. Land change in the Brazilian Savanna (Cerrado), 1986-2002: Comparative analysis and implications for land-use policy. *Land Use Policy,* 25**,** 579-595.

CENTRALBYRÅN, S. S. 2017. *Folkmängd i riket, län och kommuner 31 december 2016 och befolkningsförändringar 1 oktober–31 december 2016* [Online]. Available: https://www.scb.se/hitta-statistik/statistik-efter-amne/befolkning/befolkningens-sammansattning/befolkningsstatistik/pong/tabell-och-diagram/kvartals--och-halvarsstatistik--kommun-lan-och-riket/kvartal-4-2016/ [Accessed 22 september 2017].

CHAPIN III, F. S., ZAVALETA, E. S., EVINER, V. T. & NAYLOR, R. L. 2000. Consequences of changing biodiversity. *Nature,* 405**,** 234.

CHEN, G., HAY, G. J., CARVALHO, L. M. & WULDER, M. A. 2012. Object-based change detection. *International Journal of Remote Sensing,* 33**,** 4434-4457.

CHEN, X., VIERLING, L. & DEERING, D. 2005. A simple and effective radiometric correction method to improve landscape change detection across sensors and across time. *Remote Sensing of Environment,* 98**,** 63-79.

CHUAI, X. W., HUANG, X. J., WANG, W. J. & BAO, G. 2013. NDVI, temperature and precipitation changes and their relationships with different vegetation types during 1998–2007 in Inner Mongolia, China. *International Journal of Climatology,* 33**,** 1696-1706.

CONGALTON, R. G. & GREEN, K. 2008. *Assessing the accuracy of remotely sensed data: principles and practices*, CRC press.

CONGALTON, R. G. & PLOURDE, L. 2002. Quality assurance and accuracy assessment of information derived from remotely sensed data. *Manual of geospatial science and technology***,** 349-361.

COULTER, L. L., STOW, D. A., TSAI, Y.-H., IBANEZ, N., SHIH, H.-C., KERR, A., BENZA, M., WEEKS, J. R. & MENSAH, F. 2016. Classification and assessment of land cover and land use change in southern Ghana using dense stacks of Landsat 7 ETM+ imagery. *Remote Sensing of Environment,* 184**,** 396-409.

DASH, J., MATHUR, A., FOODY, G. M., CURRAN, P. J., CHIPMAN, J. W. & LILLESAND, T. M. 2007. Land cover classification using multi-temporal MERIS vegetation indices. *International Journal of Remote Sensing,* 28**,** 1137-1159.

DEL MAR LÓPEZ, T., AIDE, T. M. & THOMLINSON, J. R. 2001. Urban Expansion and the Loss of Prime Agricultural Lands in Puerto Rico. *AMBIO: A Journal of the Human Environment,* 30**,** 49-54.

DENG, J. S., WANG, K., DENG, Y. H. & QI, G. J. 2008. PCA-based land-use change detection and analysis using multitemporal and multisensor satellite data. *International Journal of Remote Sensing,* 29**,** 4823-4838.

DEWAN, A. M. & YAMAGUCHI, Y. 2009. Land use and land cover change in Greater Dhaka, Bangladesh: Using remote sensing to promote sustainable urbanization. *Applied Geography,* 29**,** 390-401.

DINGLE ROBERTSON, L. & KING, D. J. 2011. Comparison of pixel- and object-based classification in land cover change mapping. *International Journal of Remote Sensing,* 32**,** 1505-1529.

ECOGNITION®, T. 2016. eCognition User Guide.

EEA. 2010. *(CLC) CLC nomenclature* [Online]. Available: http://www.igeo.pt/gdr/pdf/CLC2006_nomenclature_addendum.pdf [Accessed 11-11 2017].

ESA. 2017. *Sentinel-2 - Overview - Sentinel Online* [Online]. ESA. Available: https://sentinel.esa.int/web/sentinel/missions/sentinel-2/overview [Accessed 21-10 2017].

FAZAL, S. 2000. Urban expansion and loss of agricultural land - a GIS based study of Saharanpur City, India. *Environment and Urbanization,* 12**,** 133-149.

FEARNSIDE, P. M. 2005. Deforestation in Brazilian Amazonia: History, Rates, and Consequences

Deforestación en la Amazonía Brasileña: Historia, Tasas y Consecuencias. *Conservation Biology,* 19**,** 680-688.

FOLEY, J. A., DEFRIES, R., ASNER, G. P., BARFORD, C., BONAN, G., CARPENTER, S. R., CHAPIN, F. S., COE, M. T., DAILY, G. C., GIBBS, H. K., HELKOWSKI, J. H., HOLLOWAY, T., HOWARD, E. A., KUCHARIK, C. J., MONFREDA, C., PATZ, J. A., PRENTICE, I. C., RAMANKUTTY, N. & SNYDER, P. K. 2005. Global Consequences of Land Use. *Science,* 309**,** 570-574.

GIULIANI, G., DAO, H., DE BONO, A., CHATENOUX, B., ALLENBACH, K., DE LABORIE, P., RODILA, D., ALEXANDRIS, N. & PEDUZZI, P. 2017. Live Monitoring of Earth Surface (LiMES): A framework for monitoring environmental changes from Earth Observations. *Remote Sensing of Environment,* 202**,** 222-233.

GRIMM, N. B., FAETH, S. H., GOLUBIEWSKI, N. E., REDMAN, C. L., WU, J., BAI, X. & BRIGGS, J. M. 2008. Global Change and the Ecology of Cities. *Science,* 319**,** 756-760.

HACKELOEER, A., KLASING, K., KRISP, J. M. & MENG, L. 2014. Georeferencing: a review of methods and applications. *Annals of GIS,* 20**,** 61-69.

HAYES, D. J. & SADER, S. A. 2001. Comparison of change-detection techniques for monitoring tropical forest clearing and vegetation regrowth in a time series. *Photogrammetric engineering and remote sensing,* 67**,** 1067-1075.

HE, C. Y., LIU, Z. F., TIAN, J. & MA, Q. 2014. Urban expansion dynamics and natural habitat loss in China: a multiscale landscape perspective. *Global Change Biology,* 20**,** 2886-2902.

HUSSAIN, M., CHEN, D., CHENG, A., WEI, H. & STANLEY, D. 2013. Change detection from remotely sensed images: From pixel-based to object-based approaches. *ISPRS Journal of Photogrammetry and Remote Sensing,* 80**,** 91-106.

IM, J., JENSEN, J. R. & TULLIS, J. A. 2008. Object-based change detection using correlation image analysis and image segmentation. *International Journal of Remote Sensing,* 29**,** 399-423.

IMMITZER, M., VUOLO, F. & ATZBERGER, C. 2016. First Experience with Sentinel-2 Data for Crop and Tree Species Classifications in Central Europe. *Remote Sensing,* 8**,** 166.

JIANG, L., DENG, X. & SETO, K. C. 2013. The impact of urban expansion on agricultural land use intensity in China. *Land Use Policy,* 35**,** 33-39.

JIANYA, G., HAIGANG, S., GUORUI, M. & QIMING, Z. 2008. A review of multi-temporal remote sensing data change detection algorithms. *The International Archives of the Photogrammetry, Remote Sensing and Spatial Information Sciences,* 37**,** 757-762.

KALNAY, E. & CAI, M. 2003. Impact of urbanization and land-use change on climate. *Nature,* 423**,** 528-531.

KASANKO, M., BARREDO, J. I., LAVALLE, C., MCCORMICK, N., DEMICHELI, L., SAGRIS, V. & BREZGER, A. 2006. Are European cities becoming dispersed?: A comparative analysis of 15 European urban areas. *Landscape and Urban Planning,* 77**,** 111-130.

KINDU, M., SCHNEIDER, T., TEKETAY, D. & KNOKE, T. 2013. Land use/land cover change analysis using object-based classification approach in Munessa-Shashemene landscape of the Ethiopian highlands. *Remote Sensing,* 5**,** 2411-2435.

KNORN, J., RABE, A., RADELOFF, V. C., KUEMMERLE, T., KOZAK, J. & HOSTERT, P. 2009. Land cover mapping of large areas using chain classification of neighboring Landsat satellite images. *Remote Sensing of Environment,* 113**,** 957-964.

KUEMMERLE, T., CHASKOVSKYY, O., KNORN, J., RADELOFF, V. C., KRUHLOV, I., KEETON, W. S. & HOSTERT, P. 2009. Forest cover change and illegal logging in the Ukrainian Carpathians in the transition period from 1988 to 2007. *Remote Sensing of Environment,* 113**,** 1194-1207.

LEFEBVRE, A., CORPETTI, T. & HUBERT-MOY, L. Object-oriented approach and texture analysis for change detection in very high resolution images. Geoscience and remote sensing symposium, 2008. IGARSS 2008. IEEE international, 2008. IEEE, IV-663-IV-666.

LEWIS, A., LYMBURNER, L., PURSS, M. B., BROOKE, B., EVANS, B., IP, A., DEKKER, A. G., IRONS, J. R., MINCHIN, S. & MUELLER, N. 2016. Rapid, high-resolution detection of environmental change over continental scales from satellite data–the Earth Observation Data Cube. *International Journal of Digital Earth,* 9**,** 106-111.

LI, S., DRAGICEVIC, S., CASTRO, F. A., SESTER, M., WINTER, S., COLTEKIN, A., PETTIT, C., JIANG, B., HAWORTH, J., STEIN, A. & CHENG, T. 2016. Geospatial big data handling theory and methods: A review and research challenges. *ISPRS Journal of Photogrammetry and Remote Sensing,* 115**,** 119-133.

LILLESAND, T. M., KIEFER, R. W. & CHIPMAN, J. W. 1987. Concepts and foundations of remote sensing. *Remote Sensing and Image Interpretation. John Wiley, New York***,** 1-84.

LIU, D. & XIA, F. 2010. Assessing object-based classification: advantages and limitations. *Remote Sensing Letters,* 1**,** 187-194.

LU, D., BATISTELLA, M. & MORAN, E. 2008. Integration of Landsat TM and SPOT HRG Images for Vegetation Change Detection in the Brazilian Amazon. *Photogrammetric Engineering & Remote Sensing,* 74**,** 421-430.

LU, D., MAUSEL, P., BRONDÍZIO, E. & MORAN, E. 2004. Change detection techniques. *International Journal of Remote Sensing,* 25**,** 2365-2401.

LU, D. & WENG, Q. 2007. A survey of image classification methods and techniques for improving classification performance. *International Journal of Remote Sensing,* 28**,** 823-870.

MA, Y., WU, H., WANG, L., HUANG, B., RANJAN, R., ZOMAYA, A. & JIE, W. 2015. Remote sensing big data computing: Challenges and opportunities. *Future Generation Computer Systems,* 51**,** 47-60.

MCDERMID, G. J., LINKE, J., PAPE, A. D., LASKIN, D. N., MCLANE, A. J. & FRANKLIN, S. E. 2008. Object-based approaches to change analysis and thematic map update: challenges and limitations. *Canadian Journal of Remote Sensing,* 34**,** 462-466.

MUNYATI, C. 2000. Wetland change detection on the Kafue Flats, Zambia, by classification of a multitemporal remote sensing image dataset. *International Journal of Remote Sensing,* 21**,** 1787-1806.

NASA. 2017. *The Enhanced Thematic Mapper Plus* [Online]. NASA. Available: https://landsat.gsfc.nasa.gov/the-enhanced-thematic-mapper-plus/ [Accessed October 19 2017].

NATIVI, S., MAZZETTI, P., SANTORO, M., PAPESCHI, F., CRAGLIA, M. & OCHIAI, O. 2015. Big Data challenges in building the Global Earth Observation System of Systems. *Environmental Modelling & Software,* 68**,** 1-26.

OLIVEIRA, S. F., FÜRLINGER, K. & KRANZLMÜLLER, D. Trends in computation, communication and storage and the consequences for data-intensive science. High Performance Computing and Communication & 2012 IEEE 9th International Conference on Embedded Software and Systems (HPCC-ICESS), 2012 IEEE 14th International Conference on, 2012. IEEE, 572-579.

PAOLINI, L., GRINGS, F., SOBRINO, J. A., JIMÉNEZ MUÑOZ, J. C. & KARSZENBAUM, H. 2006. Radiometric correction effects in Landsat multi-date/multi-sensor change detection studies. *International Journal of Remote Sensing,* 27**,** 685-704.

PHILIP CHEN, C. L. & ZHANG, C.-Y. 2014. Data-intensive applications, challenges, techniques and technologies: A survey on Big Data. *Information Sciences,* 275**,** 314-347.

RAWAT, J., BISWAS, V. & KUMAR, M. 2013. Changes in land use/cover using geospatial techniques: A case study of Ramnagar town area, district Nainital, Uttarakhand, India. *The Egyptian Journal of Remote Sensing and Space Science,* 16**,** 111-117.

SETO, K. C., GÜNERALP, B. & HUTYRA, L. R. 2012. Global forecasts of urban expansion to 2030 and direct impacts on biodiversity and carbon pools. *Proceedings of the National Academy of Sciences,* 109**,** 16083-16088.

SETO, K. C., PARNELL, S. & ELMQVIST, T. 2013. A global outlook on urbanization. *Urbanization, biodiversity and ecosystem services: Challenges and opportunities.* Springer.

SHALABY, A. & TATEISHI, R. 2007. Remote sensing and GIS for mapping and monitoring land cover and land-use changes in the Northwestern coastal zone of Egypt. *Applied Geography,* 27**,** 28-41.

SINGH, A. 1989. Review Article Digital change detection techniques using remotely-sensed data. *International Journal of Remote Sensing,* 10**,** 989-1003.

SKOG, K. L. & STEINNES, M. 2016. How do centrality, population growth and urban sprawl impact farmland conversion in Norway? *Land Use Policy,* 59**,** 185-196.

SONG, C. & WOODCOCK, C. E. 2003. Monitoring forest succession with multitemporal Landsat images: Factors of uncertainty. *IEEE Transactions on Geoscience and Remote Sensing,* 41**,** 2557-2567.

SONG, M., CIVCO, D. L. & HURD, J. D. 2005. A competitive pixel-object approach for land cover classification. *International Journal of Remote Sensing,* 26**,** 4981-4997.

STEHMAN, S. V. & CZAPLEWSKI, R. L. 1998. Design and Analysis for Thematic Map Accuracy Assessment: Fundamental Principles. *Remote Sensing of Environment,* 64**,** 331-344.

TAN, M., LI, X., XIE, H. & LU, C. 2005. Urban land expansion and arable land loss in China—a case study of Beijing–Tianjin–Hebei region. *Land Use Policy,* 22**,** 187-196.

TAYLOR, J. C., BREWER, T. R. & BIRD, A. C. 2000. Monitoring landscape change in the National Parks of England and Wales using aerial photo interpretation and GIS. *International Journal of Remote Sensing,* 21**,** 2737-2752.

TEHRANY, M. S., PRADHAN, B. & JEBUR, M. N. 2013. Remote sensing data reveals eco-environmental changes in urban areas of Klang Valley, Malaysia: contribution from object based analysis. *Journal of the Indian Society of Remote Sensing,* 41**,** 981-991.

TEWKESBURY, A. P., COMBER, A. J., TATE, N. J., LAMB, A. & FISHER, P. F. 2015. A critical synthesis of remotely sensed optical image change detection techniques. *Remote Sensing of Environment,* 160**,** 1-14.

THOMLINSON, J. R., BOLSTAD, P. V. & COHEN, W. B. 1999. Coordinating Methodologies for Scaling Landcover Classifications from Site-Specific to Global: Steps toward Validating Global Map Products. *Remote Sensing of Environment,* 70**,** 16-28.

TOWNSHEND, J. R., JUSTICE, C. O., GURNEY, C. & MCMANUS, J. 1992. The impact of misregistration on change detection. *IEEE Transactions on Geoscience and remote sensing,* 30**,** 1054-1060.

TURNER, B., MEYER, W. B. & SKOLE, D. L. 1994. Global land-use/land-cover change: towards an integrated study. *Ambio. Stockholm,* 23**,** 91-95.

USGS. 2015. *Landsat 7 Enhanced Thematic Mapper Plus (ETM+) Level-1 Data Products* [Online]. U.S. Department of the Interior. Available: https://lta.cr.usgs.gov/LETMP [Accessed 11-11 2017].

USGS. 2017. *Landsat Collections* [Online]. U.S. Geological Survey. [Accessed 20-10 2017].

WARD, D., PHINN, S. R. & MURRAY, A. T. 2000. Monitoring Growth in Rapidly Urbanizing Areas Using Remotely Sensed Data. *The Professional Geographer,* 52**,** 371-386.

WÄSTFELT, A. & ZHANG, Q. 2016. Reclaiming localisation for revitalising agriculture: A case study of peri-urban agricultural change in Gothenburg, Sweden. *Journal of Rural Studies,* 47**,** 172-185.

WU, Q., LI, H.-Q., WANG, R.-S., PAULUSSEN, J., HE, Y., WANG, M., WANG, B.-H. & WANG, Z. 2006. Monitoring and predicting land use change in Beijing using remote sensing and GIS. *Landscape and Urban Planning,* 78**,** 322-333.

YAN, G., MAS, J. F., MAATHUIS, B. H. P., XIANGMIN, Z. & VAN DIJK, P. M. 2006. Comparison of pixel-based and object-oriented image classification approaches—a case study in a coal fire area, Wuda, Inner Mongolia, China. *International Journal of Remote Sensing,* 27**,** 4039-4055.

YUAN, F. & BAUER, M. E. 2007. Comparison of impervious surface area and normalized difference vegetation index as indicators of surface urban heat island effects in Landsat imagery. *Remote Sensing of Environment,* 106**,** 375-386.

YUAN, F., SAWAYA, K. E., LOEFFELHOLZ, B. C. & BAUER, M. E. 2005. Land cover classification and change analysis of the Twin Cities (Minnesota) Metropolitan Area by multitemporal Landsat remote sensing. *Remote Sensing of Environment,* 98**,** 317-328.

ZANGANEH SHAHRAKI, S., SAURI, D., SERRA, P., MODUGNO, S., SEIFOLDDINI, F. & POURAHMAD, A. 2011. Urban sprawl pattern and land-use change detection in Yazd, Iran. *Habitat International,* 35**,** 521-528.

ZHANG, J., LI, P. & WANG, J. 2014. Urban Built-Up Area Extraction from Landsat TM/ETM+ Images Using Spectral Information and Multivariate Texture. *Remote Sensing,* 6**,** 7339.

ZHOU, W., TROY, A. & GROVE, M. 2008. Object-based land cover classification and change analysis in the Baltimore metropolitan area using multitemporal high resolution remote sensing data. *Sensors,* 8**,** 1613-1636.

Datasets

Figure 1 shapefiles Sweden and the world: Naturalearthdata.com. (2018). Natural Earth. [online] Available at: http://www.naturalearthdata.com, accessed [09-01-2018].

USGS, 1999, Landsat 7 ETM+, C1 Level-1, USGS Earth Resources Observation and Science (EROS) Center, Sioux Falls, South Dakota (https://lpdaac.usgs.gov), accessed [25-10-2017], at https://earthexplorer.usgs.gov/.

ESA, 2015, Sentinel 2a, Level 1C, USGS Earth Resources Observation and Science (EROS) Center, Sioux Falls, South Dakota (https://lpdaac.usgs.gov), accessed [28-10-2017], at https://earthexplorer.usgs.gov/.

Appendices

Appendix A: vegetation or agricultural lands that changed into urban areas between 1999 and 2017

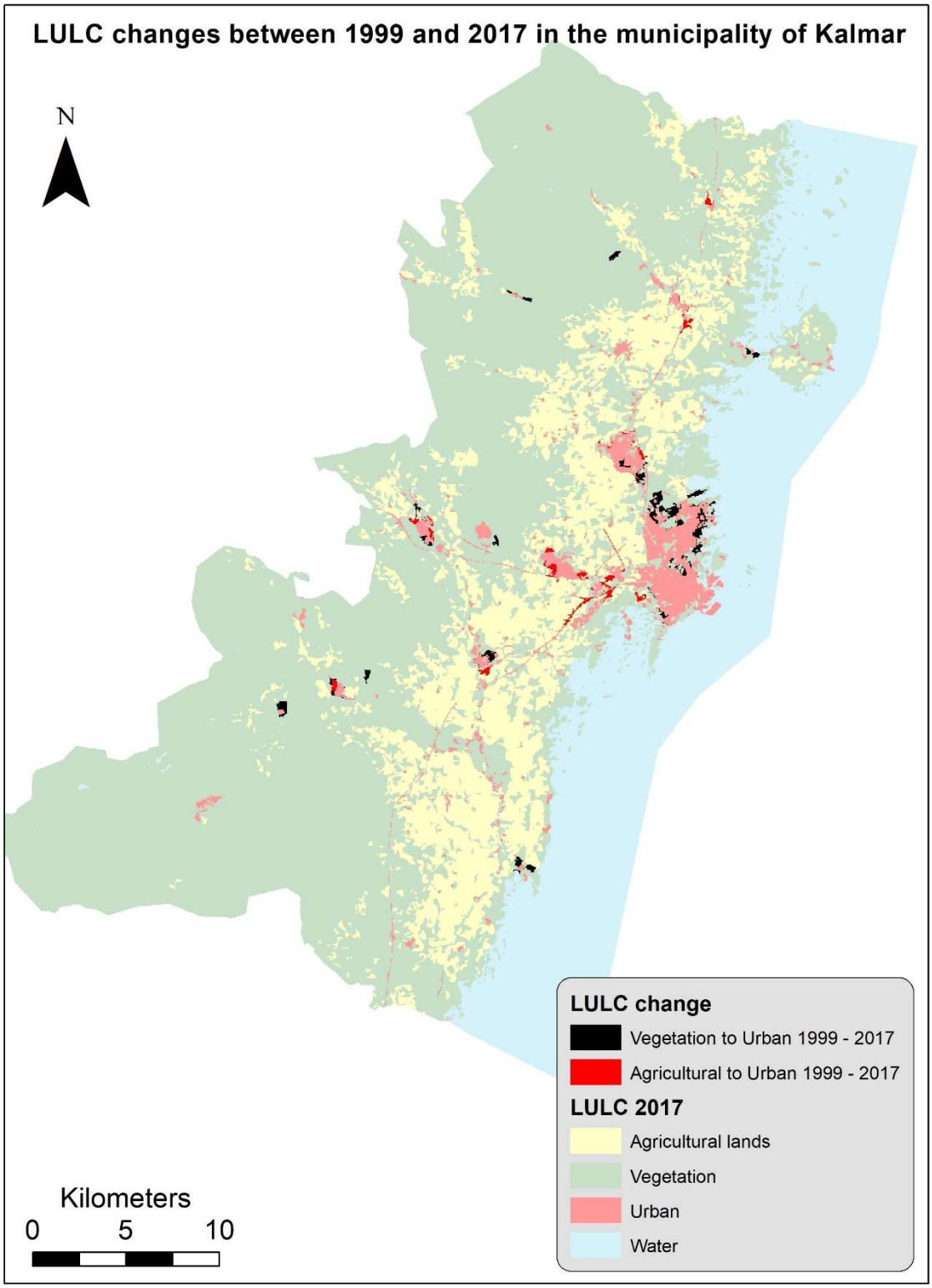

Appendix B: Unmodified from-to change map study area.